Overlapping Functions of the Yeast Oxysterol-Binding Protein Homologues

Christopher T. Beh,* Laurence Cool,† John Phillips‡ and Jasper Rine*

**Department of Molecular and Cell Biology, University of California, Berkeley, California 94720-3202, †University of California Forest Products Laboratory, Richmond, California 94804-4698 and ‡Rosetta Inpharmatics, Kirkland, Washington 98034*

Manuscript received October 5, 2000
Accepted for publication November 29, 2000

ABSTRACT

The *Saccharomyces cerevisiae* genome encodes seven homologues of the mammalian oxysterol-binding protein (OSBP), a protein implicated in lipid trafficking and sterol homeostasis. To determine the functions of the yeast OSBP gene family (*OSH1–OSH7*), we used a combination of genetics, genomics, and sterol lipid analysis to characterize *OSH* deletion mutants. All 127 combinations and permutations of *OSH* deletion alleles were constructed. Individual *OSH* genes were not essential for yeast viability, but the elimination of the entire gene family was lethal. Thus, the family members shared an essential function. In addition, the *in vivo* depletion of all Osh proteins disrupted sterol homeostasis. Like mutants that affect ergosterol production, the viable combinations of *OSH* deletion alleles exhibited specific sterol-related defects. Although none of the single *OSH* deletion mutants was defective for growth, gene expression profiles revealed that each mutant had a characteristic molecular phenotype. Therefore, each gene performed distinct nonessential functions and contributed to a common essential function. Our findings indicated that *OSH* genes performed a multitude of nonessential roles defined by specific subsets of the genes and that most shared at least one essential role potentially linked to changes in sterol lipid levels.

ERGOSTEROL, a cholesterol-like lipid, is a major constituent of the yeast cell membrane, where it is present in 3.3-fold molar excess over all phospholipids (Zinser *et al.* 1991). In eukaryotes, sterols like cholesterol and ergosterol are the bulk isoprenoid products of the mevalonate biosynthetic pathway. The products of the mevalonate pathway exert feedback regulation on their own synthesis at both transcriptional and post-transcriptional levels (Goldstein and Brown 1990; Brown and Goldstein 1997, 1999). Oxygenated derivatives of cholesterol, referred to as oxysterols, are particularly potent feedback regulators (Kandutsch *et al.* 1978). Oxysterols are biosynthetic metabolites of sterols, steroids, and bile acids and are also produced when sterols are exposed to oxidants. In addition to cholesterol feedback regulation, oxysterols play roles in apoptosis, cellular aging, platelet aggregation, and sphingolipid metabolism (reviewed in Schroepfer 2000). Two protein families appear to mediate many of the activities ascribed to oxysterols. These proteins include some of the steroid hormone nuclear receptors (reviewed by Russell 1999) and another family known as the oxysterol-binding proteins (OSBPs).

The canonical OSBP was purified to homogeneity on the basis of its high affinity for oxysterols (Dawson *et al.* 1989a) and the corresponding gene was subsequently cloned (Dawson *et al.* 1989b). Homologues are present in many eukaryotes, including humans (Levanon *et al.* 1990), flies (Alphey *et al.* 1998), worms (*C. elegans* Sequencing Consortium 1998), and fungi (Jiang *et al.* 1994; Schmalix and Bandlow 1994; Fang *et al.* 1996; Daum *et al.* 1999; Hull and Johnson 1999). Because of its binding activity and the potency of oxysterols as feedback regulators, OSBP was proposed to mediate feedback control of the mevalonate pathway (Taylor *et al.* 1984). However, the SRE binding protein (SREBP) and SREBP cleavage-activating protein (SCAP) are now known to mediate this role (reviewed by Brown and Goldstein 1997, 1999) and SREBP is unrelated in sequence to any OSBP. Nevertheless, overexpression of the mammalian OSBP gene causes pleiotropic effects on both cholesterol synthesis and expression of genes encoding some mevalonate pathway enzymes (Lagace *et al.* 1997). However, the *in vivo* role of the OSBP family is still unclear.

The localization of OSBP within cells is governed by lipids. When OSBP binds oxysterols, a conformational change in the protein occurs, allowing OSBP to translocate from cytoplasmic vesicles to the Golgi apparatus (Ridgway *et al.* 1992). The amino-terminal region of OSBP contains a pleckstrin homology (PH) domain, which binds phosphatidylinositol lipids and thereby targets the protein to Golgi membranes where these lipids are enriched (Levine and Munro 1998). OSBP localization is also sensitive to concentrations of the lipid sphingomyelin (Storey *et al.* 1998; Ridgway *et al.* 1998). Since OSBP localization is inherently linked to cellular lipid distribution, the function of OSBP likely involves some aspect of lipid maintenance in membranes.

Corresponding author: Jasper Rine, Department of Molecular and Cell Biology, Rm. 401 Barker Hall, University of California, Berkeley, CA 94720-3202. E-mail: jrine@uclink4.berkeley.edu

A *Saccharomyces cerevisiae* OSBP homologue, *KES1* (referred to here as *OSH4/KES1*), has also been implicated in the PI-dependent formation of Golgi-derived transport vesicles. Deletion of this homologue in yeast bypasses the requirement for *SEC14*, an essential gene encoding a phosphatidylinositol/phosphatidylcholine transfer protein (Fang *et al.* 1996). Since Sec14p is otherwise essential for vesicle biogenesis from the Golgi, this genetic suppression suggests that yeast OSBPs are also involved in secretion. Taken together the evidence suggests that this OSBP and perhaps its homologues affect membrane trafficking, possibly by influencing lipid distribution.

The potential roles of the OSBP family are not limited to membrane trafficking. Like oxysterols themselves, OSBPs have been implicated in a diverse variety of cellular processes. OSBP homologues may be involved in tumor metastasis (Fournier *et al.* 1999) and in cell-cycle progression (Alphey *et al.* 1998). How the OSBPs are involved in these processes is unclear.

None of the Saccharomyces OSBP homologues studied to date encode an essential gene (Jiang *et al.* 1994; Schmalix and Bandlow 1994; Fang *et al.* 1996; Daum *et al.* 1999). However, mutant strains in which some of these homologues were disrupted exhibit phenotypes similar to viable mutants defective in sterol biosynthesis (Jiang *et al.* 1994; Daum *et al.* 1999). These OSBP deletion mutants are cold sensitive and are resistant to the fungal inhibitor nystatin, whose toxicity is manifested through its binding of the yeast-specific sterol, ergosterol, in the cell membrane. In some deletion strains, sterol lipid content has also been reported to be affected (Jiang *et al.* 1994; Daum *et al.* 1999). As with its mammalian counterpart, the mechanism by which the yeast OSBP homologues affect sterols is unknown.

To understand OSBP function, we analyzed the entire family of seven OSBP homologues encoded by the *S. cerevisiae* genome. We used a combination of genetics, genomics, and lipid analysis to analyze the essential and nonessential roles of the yeast *OSH* (*o*xysterol-binding protein *h*omologue) genes. With respect to cell growth, the disruption of any single *OSH* gene caused no overt phenotype. However, single deletion mutations had unique effects on gene expression profiles, indicating that the *OSH*s performed distinct nonessential roles. Since the elimination of all *OSH* genes resulted in cell lethality, together the yeast *OSH*s also performed at least one essential function in common. Moreover, sterol lipid analysis revealed that depletion of all Osh proteins drastically perturbed sterol levels. These results indicated that, collectively, the members of the *OSH* gene family were essential for the maintenance of sterol lipid composition and for cell viability.

MATERIALS AND METHODS

Strains and microbial and genetic techniques: Culture media and genetic manipulations were as described (Adams *et al.* 1997). Yeast rich medium (YPD) was supplemented with excess tryptophan (50 mg/liter) because of tryptophan import defects of some mutants. Cycloheximide-resistant strains (*cyh2*^{R}) were selected on solid YPD containing 10 mg/liter cycloheximide. Lovastatin (a gift of James Bergstrom, Merck) was prepared as previously described (Dimster-Denk *et al.* 1994). Nystatin (Sigma Chemicals, Inc., St. Louis) was added to cooled agar medium from an ethanol stock (10 mg/ml) and the plates were used within 24 hr. To select for the *kanMX4* gene, yeast were grown on YPD containing 200 μg/ml geneticin sulfate (G418) (Gibco BRL Life Technologies, Inc., Rockville, MD; Wach *et al.* 1994). For lipid extractions, gas chromatography (GC) grade methanol and hexane were used (Fisher Scientific, Pittsburgh).

The genotypes of all yeast strains used in this article are shown in Table 1. All strains were congenic with SEY6210, unless otherwise noted. Strains bearing all permutations of gene disruptions were constructed through a systematic series of crosses. Each of the seven *OSH* deletions was marked by one of four prototrophic markers or by the *kanMX4* gene (see below).

Sequence analysis: OSBP homologues were identified using BLASTP homology searches (Altschul *et al.* 1990) of the complete yeast genome sequence (Goffeau *et al.* 1996). Sequence alignments were performed using the CLUSTALW alignment program. Kyte and Doolittle (1982) plots were used to determine protein hydrophilicity. Secondary structure predictions were determined by the method of Chou and Fasman (1978). Coiled-coil domain probability plots were generated as described by Lupas (1996), and transmembrane domains were analyzed using the TMpred program, both offered at www.ch.embnet.org/. Percentage similarity and identity between protein sequences was determined using the BESTFIT program of the GCG sequence analysis package.

The yeast genome encodes seven OSBP homologues (see results) including the gene referred to here as *OSH1*. Previously, *OSH1* had been reported as two different and separate genes, *SWH1* (Schmalix and Bandlow 1994) and *OSH1* (Jiang *et al.* 1994). *OSH1* has also been given the open reading frame designation YAR042w. However, the protein sequences of *SWH1* and *OSH1* overlap. As determined by the size of epitope-tagged versions of Osh1p detected by immunoblot (our unpublished results), the protein size was consistent with the larger protein sequence reported in EMBL/GenBank Data Library accession no. X74552.

Cloning and plasmid constructions: Restriction enzymes used for cloning were obtained from New England Biolabs (Beverly, MA), and cloning techniques were performed as described (Sambrook *et al.* 1989). To construct plasmids with which to disrupt *OSH* genes, the genes *OSH2*, *OSH3*, *OSH6*, and *OSH7* were amplified by the polymerase chain reaction (PCR) using DNA from yeast strain SEY6210 as template. Primers were designed to generate fragments with restriction sites at the ends to facilitate cloning. All disruptions and chromosomal integrations were verified by DNA blot analysis. The *osh1*Δ*::URA3*, *osh4/kes1*Δ*::HIS3*, and *osh5/hes1*Δ*::LEU2* strains HAB835, HAB821, and HAB826, respectively (Jiang *et al.* 1994), were gifts of Howard Bussey (McGill University).

To construct the *osh7*Δ*::HIS3* disruption plasmid (pJR2281), the primer combinations used were: 5′-GCTAGGATCCA GTTCTCATAGCTCAATTAACG-3′ and 5′-CAGTGGATCCTT CAGGGATGTGCTTG-3′. The 1.2-kb fragment was cloned into the *Bam*HI site of pBluescript KS(+)(pBS-KS+; Stratagene, La Jolla, CA). From this plasmid, a 510-bp *Bam*HI-*Eco*RI fragment and a 160-bp *Bam*HI-*Xba*I fragment were subcloned into the *Eco*RI-*Xba*I sites of pRS403 (Sikorski and Hieter 1989) to generate pJR2281. To integrate and disrupt *OSH7*, pJR2281 was digested with *Bam*HI and the entire plas-

TABLE 1

Yeast strains used

Strain	Genotype	Origin[a]
CBX2	SEY6210 *cyh2* [GRM1-96][b]	
CBX6	SEY6210 *cyh2 osh4Δ::HIS3* [GRM1-96, *URA3*][b]	
CBX7	SEY6210 *cyh2 osh7Δ::HIS3* [GRM1-96, *URA3*][b]	
CBX9	SEY6210 *cyh2 osh5Δ::LEU2* [GRM1-96, *URA3*][b]	
CBX10	SEY6210 *cyh2 osh6Δ::LEU2* [GRM1-96, *URA3*][b]	
CBX11	SEY6210 *cyh2 osh3Δ::LYS2* [GRM1-96, *URA3*][b]	
CBX12	SEY6210 *cyh2 osh2Δ::kan-MX4* [GRM1-96, *URA3*][b]	
CBX13	*MAT*α *cyh2 ura3Δ::kan-MX4 his3Δ200 lys2-801 leu2-3,112 trp1Δ901 suc2Δ9* [GRM1-96, *URA3*][b]	
CBX14	SEY6210 *chy2 osh1Δ::kan-MX4* [GRM1-96, *URA3*][b]	
CBX20	*MAT*α *chy2 ura3-52 lys2-801 leu2-3,112 trp1Δ901 suc2Δ9* [GRM1-96, *URA3*][b]	
CBX21	*MAT*α *cyh2 ura3-52 his3Δ200 lys2-801 trp1Δ901 suc2Δ9* [GRM1-96, *URA3*][b]	
CBX22	*MAT*α *cyh2 ura3-52 his3Δ200 leu2-3,112 trp1Δ901 suc2Δ9* [GRM1-96, *URA3*][b]	
CTY1-1A	*MAT***a** *ura3-52 his3Δ200 lys2-801 sec14-1*	Bankaitis *et al.* (1989)
HAB821	SEY6210 *osh4Δ/kes1Δ::HIS3*	Jiang *et al.* (1994)
HAB835	SEY6210 *osh1Δ::URA3*	Jiang *et al.* (1994)
JRY6200	SEY6210 *osh7Δ::HIS3*	
JRY6201	SEY6210 *osh6Δ::LEU2*	
JRY6202	SEY6210 *osh3Δ::LYS2*	
JRY6203	SEY6210 *osh2Δ::URA3*	
JRY6206	SEY6210 *osh5Δ/hes1Δ::LEU2*	
JRY6207	SEY6210 *osh6Δ::LEU2 osh7Δ::HIS3*	
JRY6208	SEY6210 *osh3Δ::LYS2 osh7Δ::HIS3*	
JRY6209	SEY6210 *osh2Δ::URA3 osh7Δ::HIS3*	
JRY6210	SEY6210 *osh1Δ::URA3 osh7Δ::HIS3*	
JRY6211	SEY6210 *osh4Δ::HIS3 osh7Δ::HIS3*	
JRY6212	SEY6210 *osh5Δ::LEU2 osh7Δ::HIS3*	
JRY6213	SEY6210 *osh3Δ::LYS2 osh6Δ::LEU2*	
JRY6214	SEY6210 *osh2Δ::URA3 osh6Δ::LEU2*	
JRY6215	SEY6210 *osh1Δ::URA3 osh6Δ::LEU2*	
JRY6216	SEY6210 *osh4Δ::HIS3 osh6Δ::LEU2*	
JRY6217	SEY6210 *osh5Δ::LEU2 osh6Δ::LEU2*	
JRY6218	SEY6210 *osh2Δ::URA3 osh3Δ::LYS2*	
JRY6219	SEY6210 *osh1Δ::URA3 osh3Δ::LYS2*	
JRY6220	SEY6210 *osh3Δ::LYS2 osh4ΔHIS3*	
JRY6221	SEY6210 *osh3Δ::LYS2 osh5Δ::LEU2*	
JRY6222	SEY6210 *osh1Δ::URA3 osh2Δ::URA3*	
JRY6223	SEY6210 *osh2Δ::URA3 osh4Δ::HIS3*	
JRY6224	SEY6210 *osh2Δ::URA3 osh5Δ::LEU2*	
JRY6225	SEY6210 *osh1Δ::URA3 osh4Δ::HIS3*	
JRY6226	SEY6210 *osh1Δ::URA3 osh5Δ::LEU2*	
JRY6227	SEY6210 *osh4Δ::HIS3 osh5Δ::LEU2*	
JRY6228	SEY6210 *osh3Δ::LYS2 osh6Δ::LEU2 osh7Δ::HIS3*	
JRY6229	SEY6210 *osh2Δ::URA3 osh6Δ::LEU2 osh7Δ::HIS3*	
JRY6230	SEY6210 *osh1Δ::URA3 osh6Δ::LEU2 osh7Δ::HIS3*	
JRY6231	SEY6210 *osh4Δ::HIS3 osh6Δ::LEU2 osh7Δ::HIS3*	
JRY6232	SEY6210 *osh5Δ::LEU2 osh6Δ::LEU2 osh7Δ::HIS3*	
JRY6233	SEY6210 *osh2Δ::URA3 osh3Δ::LYS2 osh7Δ::HIS3*	
JRY6234	SEY6210 *osh1Δ::URA3 osh3Δ::LYS2 osh7Δ::HIS3*	
JRY6235	SEY6210[c] *osh3Δ::LYS2 osh4Δ::HIS3 osh7Δ::HIS3*	
JRY6236	SEY6210[c] *osh3Δ::LYS2 osh5Δ::LEU2 osh7Δ::HIS3*	
JRY6237	SEY6210 *osh1Δ::URA3 osh2Δ::URA3 osh7Δ::HIS3*	
JRY6238	SEY6210 *osh2Δ::URA3 osh4Δ::HIS3 osh7Δ::HIS3*	
JRY6239	SEY6210 *osh2Δ::URA3 osh5Δ::LEU2 osh7Δ::HIS3*	
JRY6240	SEY6210 *osh1Δ::URA3 osh4Δ::HIS3 osh7Δ::HIS3*	
JRY6241	SEY6210 *osh1Δ::URA3 osh5Δ::LEU2 osh7Δ::HIS3*	
JRY6242	SEY6210 *osh4Δ::HIS3 osh5Δ::LEU2 osh7Δ::HIS3*	
JRY6243	SEY6210 *osh2Δ::URA3 osh3Δ::LYS2 osh6Δ::LEU2*	
JRY6244	SEY6210 *osh1Δ::URA3 osh3Δ::LYS2 osh6Δ::LEU2*	
JRY6245	SEY6210 *osh3Δ::LYS2 osh4Δ::HIS3 osh6Δ::LEU2*	

(*continued*)

TABLE 1

(Continued)

Strain	Genotype	Origin
JRY6246	SEY6210 *osh3Δ::LYS2 osh5Δ::LEU2 osh6Δ::LEU2*	
JRY6247	SEY6210 *osh1Δ::URA3 osh2Δ::URA3 osh6Δ::LEU2*	
JRY6248	SEY6210 *osh2Δ::URA3 osh4Δ::HIS3 osh6Δ::LEU2*	
JRY6249	SEY6210 *osh2Δ::URA3 osh5Δ::LEU2 osh6Δ::LEU2*	
JRY6250	SEY6210[c] *osh1Δ::URA3 osh4Δ::HIS3 osh6Δ::LEU2*	
JRY6251	SEY6210 *osh1Δ::URA3 osh5Δ::LEU2 osh6Δ::LEU2*	
JRY6252	SEY6210 *osh4Δ::HIS3 osh5Δ::LEU2 osh6Δ::LEU2*	
JRY6253	SEY6210 *osh1Δ::URA3 osh2Δ::URA3 osh3Δ::LYS2*	
JRY6254	SEY6210 *osh2Δ::URA3 osh3Δ::LYS2 osh4Δ::HIS3*	
JRY6255	SEY6210 *osh2Δ::URA3 osh3Δ::LYS2 osh5Δ::LEU2*	
JRY6256	SEY6210[c] *osh1Δ::URA3 osh3Δ::LYS2 osh4Δ::HIS3*	
JRY6257	SEY6210 *osh1Δ::URA3 osh3Δ::LYS2 osh5Δ::LEU2*	
JRY6258	SEY6210 *osh3Δ::LYS2 osh4Δ::HIS3 osh5Δ::LEU2*	
JRY6259	SEY6210 *osh1Δ::URA3 osh2Δ::URA3 osh4Δ::HIS3*	
JRY6260	SEY6210 *osh1Δ::URA3 osh2Δ::URA3 osh5Δ::LEU2*	
JRY6261	SEY6210 *osh2Δ::URA3 osh4Δ::HIS3 osh5Δ::LEU2*	
JRY6262	SEY6210[c] *osh1Δ::URA3 osh4Δ::HIS3 osh5Δ::LEU2*	
JRY6263	SEY6210 *osh2Δ::URA3 osh3Δ::LYS2 osh6Δ::LEU2 osh7Δ::HIS3*	
JRY6264	SEY6210 *osh1Δ::URA3 osh3Δ::LYS2 osh6Δ::LEU2 osh7Δ::HIS3*	
JRY6265	SEY6210 *osh3Δ::LYS2 osh4Δ::HIS3 osh6Δ::LEU2 osh7Δ::HIS3*	
JRY6266	SEY6210 *osh3Δ::LYS2 osh5Δ::LEU2 osh6Δ::LEU2 osh7Δ::HIS3*	
JRY6267	SEY6210 *osh1Δ::URA3 osh2Δ::URA3 osh6Δ::LEU2 osh7Δ::HIS3*	
JRY6268	SEY6210[c] *osh2Δ::URA3 osh4Δ::HIS3 osh6Δ::LEU2 osh7Δ::HIS3*	
JRY6269	SEY6210[c] *osh2Δ::URA3 osh5Δ::LEU2 osh6Δ::LEU2 osh7Δ::HIS3*	
JRY6270	SEY6210[c] *osh1Δ::URA3 osh4Δ::HIS3 osh6Δ::LEU2 osh7Δ::HIS3*	
JRY6271	SEY6210[c] *osh1Δ::URA3 osh5Δ::LEU2 osh6Δ::LEU2 osh7Δ::HIS3*	
JRY6272	SEY6210 *osh4Δ::HIS3 osh5Δ::LEU2 osh6Δ::LEU2 osh7Δ::HIS3*	
JRY6273	SEY6210 *osh1Δ::URA3 osh2Δ::URA3 osh3Δ::LYS2 osh7Δ::HIS3*	
JRY6274	SEY6210 *osh2Δ::URA3 osh3Δ::LYS2 osh4Δ::HIS3 osh7Δ::HIS3*	
JRY6275	SEY6210 *osh2Δ::URA3 osh3Δ::LYS2 osh5Δ::LEU2 osh7Δ::HIS3*	
JRY6276	SEY6210 *osh1Δ::URA3 osh3Δ::LYS2 osh4Δ::HIS3 osh7Δ::HIS3*	
JRY6277	SEY6210 *osh1Δ::URA3 osh3Δ::LYS2 osh5Δ::LEU2 osh7Δ::HIS3*	
JRY6278	SEY6210 *osh3Δ::LYS2 osh4Δ::HIS3 osh5Δ::LEU2 osh7Δ::HIS3*	
JRY6279	SEY6210[c] *osh1Δ::URA3 osh2Δ::URA3 osh4Δ::HIS3 osh7Δ::HIS3*	
JRY6280	SEY6210 *osh1Δ::URA3 osh2Δ::URA3 osh5Δ::LEU2 osh7Δ::HIS3*	
JRY6281	SEY6210 *osh2Δ::URA3 osh4Δ::HIS3 osh5Δ::LEU2 osh7Δ::HIS3*	
JRY6282	SEY6210 *osh1Δ::URA3 osh4Δ::HIS3 osh5Δ::LEU2 osh7Δ::HIS3*	
JRY6283	SEY6210 *osh1Δ::URA3 osh2Δ::URA3 osh3Δ::LYS2 osh6Δ::LEU2*	
JRY6284	SEY6210 *osh2Δ::URA3 osh3Δ::LYS2 osh4Δ::HIS3 osh6Δ::LEU2*	
JRY6285	SEY6210 *osh2Δ::URA3 osh3Δ::LYS2 osh5Δ::LEU2 osh6Δ::LEU2*	
JRY6286	SEY6210[c] *osh1Δ::URA3 osh3Δ::LYS2 osh4Δ::HIS3 osh6Δ::LEU2*	
JRY6287	SEY6210 *osh1Δ::URA3 osh3Δ::LYS2 osh5Δ::LEU2 osh6Δ::LEU2*	
JRY6288	SEY6210 *osh3Δ::LYS2 osh4Δ::HIS3 osh5Δ::LEU2 osh6Δ::LEU2*	
JRY6289	SEY6210 *osh1Δ::URA3 osh2Δ::URA3 osh4Δ::HIS3 osh6Δ::LEU2*	
JRY6290	SEY6210 *osh1Δ::URA3 osh2Δ::URA3 osh5Δ::LEU2 osh6Δ::LEU2*	
JRY6291	SEY6210 *osh2Δ::URA3 osh4Δ::HIS3 osh5Δ::LEU2 osh6Δ::LEU2*	
JRY6292	SEY6210 *osh1Δ::URA3 osh4Δ::HIS3 osh5Δ::LEU2 osh6Δ::LEU2*	
JRY6293	SEY6210 *osh1Δ::URA3 osh2Δ::URA3 osh3Δ::LYS2 osh4Δ::HIS3*	
JRY6294	SEY6210 *osh1Δ::URA3 osh2Δ::URA3 osh3Δ::LYS2 osh5Δ::LEU2*	
JRY6295	SEY6210 *osh2Δ::URA3 osh3Δ::LYS2 osh4Δ::HIS3 osh5Δ::LEU2*	
JRY6296	SEY6210 *osh1Δ::URA3 osh3Δ::LYS2 osh4Δ::HIS3 osh5Δ::LEU2*	
JRY6297	SEY6210 *osh1Δ::URA3 osh2Δ::URA3 osh4Δ::HIS3 osh5Δ::LEU2*	
JRY6298	SEY6210 *osh1Δ::URA3 osh2Δ::URA3 osh3Δ::LYS2 osh6Δ::LEU2 osh7Δ::HIS3*	
JRY6299	SEY6210[c] *osh2Δ::URA3 osh3Δ::LYS2 osh4Δ::HIS3 osh6Δ::LEU2 osh7Δ::HIS3*	
JRY6300	SEY6210 *osh2Δ::URA3 osh3Δ::LYS2 osh5Δ::LEU2 osh6Δ::LEU2 osh7Δ::HIS3*	
JRY6301	SEY6210 *osh1Δ::URA3 osh3Δ::LYS2 osh4Δ::HIS3 osh6Δ::LEU2 osh7Δ::HIS3*	
JRY6302	SEY6210 *osh1Δ::URA3 osh3Δ::LYS2 osh5Δ::LEU2 osh6Δ::LEU2 osh7Δ::HIS3*	
JRY6303	SEY6210[c] *osh3Δ::LYS2 osh4Δ::HIS3 osh5Δ::LEU2 osh6Δ::LEU2 osh7Δ::HIS3*	

(*continued*)

TABLE 1

(Continued)

Strain	Genotype	Origin
JRY6304	SEY6210 *osh1Δ::URA3 osh2Δ::URA3 osh4Δ::HIS3 osh6Δ::LEU2 osh7Δ::HIS3*	
JRY6305	SEY6210[c] *osh1Δ::URA3 osh2Δ::URA3 osh5Δ::LEU2 osh6Δ::LEU2 osh7Δ::HIS3*	
JRY6306	SEY6210[c] *osh2Δ::URA3 osh4Δ::HIS3 osh5Δ::LEU2 osh6Δ::LEU2 osh7Δ::HIS3*	
JRY6307	SEY6210[c] *osh1Δ::URA3 osh4Δ::HIS3 osh5Δ::LEU2 osh6Δ::LEU2 osh7Δ::HIS3*	
JRY6308	SEY6210 *osh1Δ::kan-MX4 osh2Δ::URA3 osh3Δ::LYS2 osh4Δ::HIS3 osh7Δ::HIS3*	
JRY6309	SEY6210 *osh1Δ::URA3 osh2Δ::URA3 osh3Δ::LYS2 osh5Δ::LEU2 osh7Δ::HIS3*	
JRY6310	SEY6210 *osh2Δ::URA3 osh3Δ::LYS2 osh4Δ::HIS3 osh5Δ::LEU2 osh7Δ::HIS3*	
JRY6311	SEY6210 *osh1Δ::URA3 osh3Δ::LYS2 osh4Δ::HIS3 osh5Δ::LEU2 osh7Δ::HIS3*	
JRY6312	SEY6210 *osh1Δ::URA3 osh2Δ::URA3 osh4Δ::HIS3 osh5Δ::LEU2 osh7Δ::HIS3*	
JRY6313	SEY6210 *osh1Δ::URA3 osh2Δ::URA3 osh3Δ::LYS2 osh4Δ::HIS3 osh6Δ::LEU2*	
JRY6314	SEY6210 *osh1Δ::URA3 osh2Δ::URA3 osh3Δ::LYS2 osh5Δ::LEU2 osh6Δ::LEU2*	
JRY6315	SEY6210 *osh2Δ::URA3 osh3Δ::LYS2 osh4Δ::HIS3 osh5Δ::LEU2 osh6Δ::LEU2*	
JRY6316	SEY6210 *osh1Δ::URA3 osh3Δ::LYS2 osh4Δ::HIS3 osh5Δ::LEU2 osh6Δ::LEU2*	
JRY6317	SEY6210 *osh1Δ::URA3 osh2Δ::URA3 osh4Δ::HIS3 osh5Δ::LEU2 osh6Δ::LEU2*	
JRY6318	SEY6210 *osh1Δ::URA3 osh2Δ::URA3 osh3Δ::LYS2 osh4Δ::HIS3 osh5Δ::LEU2*	
JRY6319	SEY6210 *osh1Δ::kan-MX4 osh2Δ::kan-MX4 osh3Δ::LYS osh4Δ::HIS3 osh6Δ::LEU2 osh7Δ::HIS3*	
JRY6320	SEY6210[c] *osh1Δ::URA3 osh2Δ::URA3 osh3Δ::LYS2 osh5Δ::LEU2 osh6Δ::LEU2 osh7Δ::HIS3*	
JRY6321	SEY6210 *TRP1::P^{MET3}-OSH2 osh2Δ::kan-MX4 osh3Δ::LYS2 osh4Δ::HIS3 osh5Δ::LEU2 osh6Δ::LEU2 osh7Δ::HIS3*	
JRY6322	SEY6210[c] *osh1Δ::URA3 osh3Δ::LYS2 osh4Δ::HIS3 osh5Δ::LEU2 osh6Δ::LEU2 osh7Δ::HIS3*	
JRY6323	SEY6210 *osh1Δ::URA3 osh2Δ::kan-MX4 osh4Δ::HIS3 osh5Δ::LEU2 osh6Δ::LEU2 osh7Δ::HIS3*	
JRY6324	SEY6210 *osh1Δ::URA3 osh2Δ::URA3 osh3Δ::LYS2 osh4Δ::HIS3 osh5Δ::LEU2 osh7Δ::HIS3*	
JRY6325	SEY6210 *osh1Δ::URA3 osh2Δ::URA3 osh3Δ::LYS2 osh4Δ::HIS3 osh5Δ::LEU2 osh6Δ::LEU2*	
JRY6326	SEY6210 *TRP1::P^{MET3}-OSH2 osh1Δ::kan-MX4 osh3Δ::kan-MX4 osh3Δ::LYS2 osh4Δ::HIS3 osh5Δ::LEU2 osh6Δ::LEU2 osh7Δ::HIS3*	
MS2339	*MAT***a** *ura3-52 leu2-3,112 kar1-1*	Vallen *et al.* (1992)
SEY6210	*MAT*α *ura3-52 his3Δ200 lys2-801 leu2-3,112 trp1Δ901 suc2Δ9*	Robinson *et al.* (1988)

[a] Unless otherwise stated, all strains were created as part of this study.
[b] [GRM1-96] indicates the GFP reporter matrix plasmids listed in Table 2.
[c] *MAT***a** isolates that are otherwise SEY6210 isogenic.

mid was transformed into SEY6210. In the *osh7Δ* allele, 484 bp of the *OSH7* coding region were removed and replaced with the *HIS3* gene.

The oligonucleotide primers used to generate the *osh6Δ::LEU2* plasmid (pJR2282) were 5′-GCTAGGATCCTGCTGGGTTCTG CTTTTCGT-3′ and 5′-CAGTGGATCCGCGTGTAGCGACATT TTAC-3′. The 1.6-kb amplified fragment was cloned into the *Bam*HI site of pBS-KS+. From this plasmid, a 220-bp *Bam*HI-*Xho*I fragment and a 785-bp *Bam*HI-*Xba*I fragment were subcloned into the *Xho*I-*Xba*I sites of pRS405 (Sikorski and Hieter 1989), generating the plasmid pJR2282. To integrate the disruption construct, pJR2282 was digested with *Bam*HI and the entire plasmid was transformed into SEY6210. The deletion of *OSH6* removed 86 bp of upstream sequence and the first 547 bp of coding sequence.

The 2.8-kb *OSH3* fragment was amplified and cloned into the *Spe*I sites of pBS-KS+. *OSH3* was amplified using the following two primers: 5′-GCTAACTAGTCCAGTGTAGATG ACCATGC-3′ and 5′-CAGTACTAGTAACTCTTCGGTCCAGT TATG-3′. The *osh3Δ::LYS2* integration construct was produced by inserting the 360-bp *Spe*I-*Eco*RI and 240-bp *Hin*dIII-*Cla*I *OSH3* fragments from the pBS-KS+ plasmid, together with the 4.8-kb *Eco*RI-*Hin*dIII *LYS2* fragment from YIp600 (Barnes and Thorner 1986), into the *Spe*I-*Cla*I sites of pBS-KS+. The generated plasmid, pJR2283, was digested with *Spe*I and *Cla*I to integrate the 5.4-kb nonvector fragment and disrupt *OSH3*. In the *osh3Δ* allele constructed, 1.65 kb of sequence was deleted and replaced with the *LYS2* gene.

The 3.8-kb *OSH2* DNA was amplified and cloned into the *Eco*RI-*Sal*I sites of pBS-KS+. The oligonucleotide pair used for PCR was 5′-CTCGAATTCATGTCTAGGGAAGACTTG TCC-3′ and 5′-ACGCGTCGACCGTGTTAAAAAATGTCACCA CAATC-3′. From pJR987, a *Pvu*II-*Sph*I fragment containing *URA3* was subcloned into the *Sna*BI-*Sph*I sites of *OSH2* in pBS-KS+. This disruption plasmid, pJR2287, was digested with *Eco*RI and *Sal*I to integrate and delete *OSH2*. In the deletion of *OSH2*, 1.45 kb of *OSH2* coding sequence was removed and replaced with the *URA3* gene.

In some *osh1Δ* and *osh2Δ* strains, the prototrophic marker was converted from *URA3* to *kanMX4*. In these strains, the *URA3* gene was replaced with *kanMX4* using the disruption construct pJR2284. The construction of pJR2284 was made by first inserting a *Bgl*II-*Sac*I *kanMX4* fragment from pFA6a-*kanMX4* (Wach *et al.* 1994) into the *Bam*HI-*Sac*I sites of pBS-KS+. Then, into *Acc*I-*Apa*I sites of this plasmid, a 565-bp *Not*I-*Apa*I fragment and a 525-bp *Not*I-*Acc*I *URA3* fragment were inserted representing the 5′- and 3′-ends of the gene, respectively. To replace *URA3* with *kanMX4*, pJR2284 was digested with *Not*I and the entire linearized plasmid was transformed into yeast. Transformants resistant to Geneticin (G148) and 5-fluoroorotic acid (Boeke *et al.* 1984) were selected.

To generate an allele of *OSH2* under regulated control of the *MET3* promoter, the plasmid pJR2285 was constructed. In pJR2285, the *Eco*RI-*Pvu*II fragment from pJR2286, containing the *OSH2* open reading frame, replaced the *Eco*RI-*Mse*I *RAS2* fragment from pJR1786. In addition to the P^{MET3}-

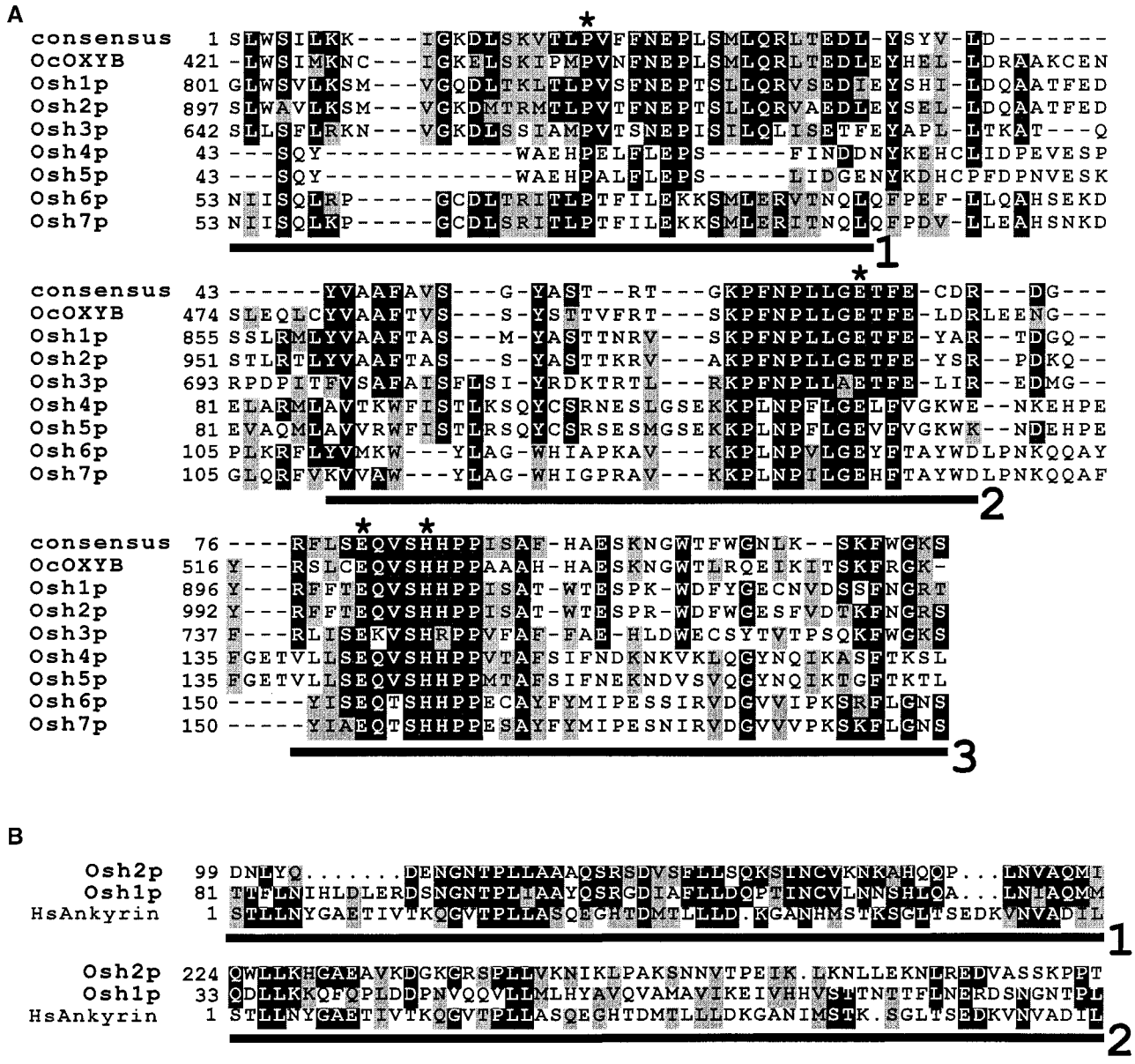

FIGURE 1.—Sequence alignments of the 7 yeast OSBP homologues compared to other related proteins. (A) Alignment of amino acid sequences from all yeast OSBP homologues (Osh1p–7p), OXYB, and the consensus sequence compiled from 39 independent OSBP homologues. The 39 OSBP homologues included the following: (*A. thalius*) At2g31020, At2g31030, At4g08180, At4g12460, At4g22540, At4g25850, At4g25860, F3F19.19, F3L24.17; (*Candida albicans*) OBPa, OBPalpha; (*C. elegans*) C32F10.1, F14H8.1, Y47D3A.17, ZK1086.1; (*D. melanogaster*) Cg1513, Cg3860, *D.m.*OSBP; (*H. sapiens*) BAA91118.1, BAA91496.1, DJ430N08.1, KIAA0704, KIAA0772, *H.s.*OXYB; (*Mus musculus*) *M.m.*OSBP; (*N. crassa*) osbP; (*Oryclolagus cuniculus*) *O.c.*OXYB; (*S. cerevisiae*) see RESULTS; (*S. pombe*) SPAC23H4.01c, SPBC1271.12, SPBC2F12.05c, SPBC354.07c, SPCC23B6.01c. Each residue in the consensus represented the amino acid found in at least 90% of OSBP homologues at that position. Solid boxes indicated identity and shaded boxes indicated similarity between a majority of aligned amino acids. Residues identified by an asterisk (*) signified invariant amino acids found in all 39 OSBP homologues. The bars (1–3) indicated OSBP subdomains within which the greatest

OSH2 promoter fusion, pJR2285 encoded *TRP1* and, after linearizing with a *Bst*XI partial digest, the construct could be integrated at sequences adjacent to *trp1Δ901*. Potential transformants were selected on plates containing solid synthetic medium without tryptophan. In the absence of methionine, the *TRP1*-integrated P^{MET3}-*OSH2* construct suppressed the lethality of a strain lacking all *OSH* genes. In medium supplemented with 100 mg/liter methionine, the P^{MET3}-*OSH2* construct could not rescue an *osh1Δ-7Δ* strain, indicating that the promoter was sufficiently repressed by methionine to deny cells the essential function of the *OSH* genes.

Reporter gene analysis: The construction of the 96 plasmids containing the green fluorescent protein (GFP) fused in frame to 96 different open reading frames, and fluorescence detection and analysis is described by Dimster-Denk *et al.* (1999). The 96 plasmids were transformed into a *kar1-1* strain (MS2339) and at least 10 independent transformants were pooled and then inoculated onto solid medium made with 0.5% agarose. These plates were made with solid synthetic complete medium (SC-Ura) and were supplemented with 50 mg/liter tryptophan. The arrayed transformants were grown at 30°.

The 96 plasmids were transferred to each of the seven deletion strains and their controls by exceptional cytoduction (Dutcher 1981) producing the CBX strain series (see Table 1). The plasmids were efficiently introduced into all recipient strains from an original set of *kar1-1* transformants. Recipient strains were grown on plates as a lawn and replica-printed onto plates with the *kar1-1* donor strains. Mating occurred on solid YPD at 30° for 6–10 hr after which plasmid transfer was selected on SC-Ura containing 3 mg/liter cycloheximide. Multiple papillae (>20) from each recipient were resuspended in sterile water and reapplied onto SC-Ura with cycloheximide.

Gene expression was normalized to the corresponding wild-type strain with matching prototrophies. A set of Osh^+ control strains was used in which each was paired for analysis with the appropriate *oshΔ* mutant strains bearing identical prototrophic markers to avoid marker effects on gene expression. In general, differences between profiles of the various prototrophic wild-type strains were nominal, indicating that marker differences contributed insignificantly to any profile similarities between *OSH* mutants.

For each plasmid in each strain, GFP fluorescence was averaged from at least 16 measurements. Pairwise profile comparisons between normalized expression ratios from each *OSH* deletion mutant were quantified by correlation coefficients, *r*. The significance of *r* was determined by the test statistic *t* (where $t = r[(n-2)/(1-r^2)]^{0.5}$ and *n* is the number of data pairs for which there was a twofold or greater effect for at least one *OSH* mutant strain). Using Student's *t*-distribution, the probability of *t* at $n-2$ d.f. was determined at a 99% confidence level. Color representations of gene expression were produced using the Dot Display program (Tod Flak, personal communication).

Sterol lipid analysis: Sterol lipids were saponified and extracted using a modification of a published method (Hampton and Rine 1994). For duplicate analysis of the same culture, 200 ml of exponentially growing yeast (0.6 to 1.0 OD_{600}) were split into two equal volumes and harvested by centrifugation. The cells were washed once with an equal volume of distilled water. Pellets were resuspended in 2.5 ml 0.1 M HCl and placed in a boiling water bath for 20 min. After centrifugation, cells were washed twice with 5 ml distilled water and then the cell pellets were resuspended in 0.5 ml 67% methanol. Glass beads were added to the mixture, and cells were lysed by vortexing twice for 3 min each. To the glass bead slurry, 2.5 ml methanol and 1.25 ml 60% KOH were added, and the suspension was heated at 70° for 90 min. Free sterols were isolated with four 2.5-ml hexane extractions after which 0.5 g anhydrous Na_2SO_4 (Sigma) was added to the pooled extracts.

Within the extracts, the identity of sterol lipids present was determined by tandem gas chromatography-mass spectroscopy (GC-MS) and the amount of each sterol was determined by quantitative GC. As an internal standard, 50 μl of a 1.00 mg/ml solution of cholesterol (Sigma) in ether was added to each hexane extract. The solvent was then evaporated at ~40° under a stream of N_2, and the residue was dissolved in ~100 μl CH_2Cl_2. The quantitative measurement of underivatized sterol was performed using GC, with flame ionization detection, under these conditions: injector temperature 280°, splitless injection (1.5 min); column 5% phenyl-95% methylpolysiloxane WCOT capillary, 0.25 mm ID × 30 m; temperature program 180° (1.5 min isothermal), to 240° at 20°/min, to 300° at 3°/min, 10-min hold at 300°; carrier gas He at 0.84 kg/cm^2; detector temperature 300°. Individual compounds were quantified from peak area ratios compared to the internal standard peak, with the assumption of equal 1.0 response factors for all sterols. To ensure accuracy, duplicate injections of each sample were performed. Using GC-MS, individual underivatized sterols were identified by retention time and/or MS comparison with literature data (Bard *et al.* 1977; Nes *et al.* 1989; NBS EPA/NIH Mass Spectral Data Base) or, in the case of ergosterol, with an authentic sample. GC conditions were the same as those used for quantitative analysis; MS detection was by electron impact at 70 eV.

Sterol lipid content was calculated either as a function of culture optical density (OD) or normalized to protein mass. For the samples in which sterol content was normalized to OD_{600}, optical density and cell size were shown to be equivalent for all the strains tested by plating dilutions of equal OD_{600} of cells on solid rich medium and counting the colonies formed. Yeast cells depleted of Osh proteins, however, were significantly larger than wild-type cells. Therefore, comparisons between sterol content of wild-type and Oshp depleted cells were calculated relative to cytosolic protein concentration. For protein determination, 0.5 ml of culture was pelleted, resuspended in 0.25 ml water, glass beads were added, and cells were then lysed by vortexing for 3 min. Insoluble debris was discarded after centrifugation in a microcentrifuge. Protein concentration was determined by Bradford assay using bovine serum albumin (Sigma) as standard. The data for each analysis represented an average of at least four measurements.

RESULTS

The OSBP superfamily of genes: To define and identify OSBP homologues, the protein sequence of the first-identified OSBP, rabbit OXYB, was used in sequence

sequence identity between OSBP homologues was located. The three subdomains were separated by regions less conserved in sequence and in length. (B) Alignment of the ankryin repeat domains of Osh2p and Osh1p with human Ankyrin-2. The N-terminal regions of both Osh2p and Osh1p contained two motifs with similarity to ankyrin repeats. The motifs from Osh2p and Osh1p with the highest similarity to the canonical ankyrin repeat are indicated by the bar numbered 1. The second, less homologous repeats of Osh2p and Osh1p are indicated with bar numbered 2. (C) The pleckstrin homology (PH) domains of Osh3p, Osh2p, Osh1p, and OXYB, aligned with mouse pleckstrin-2.

	OSH1	*OSH2*	*OSH3*	*OSH4*	*OSH5*	*OSH6*	*OSH7*
OXYB	34.4(54.8)	33.4(53.4)	29.1(48.1)	22.9(44.6)	21.5(43.2)	21.5(45.7)	21.3(45.5)
OSH7	25.8(50.1)	26.6(50.6)	25.3(44.2)	29.8(51.9)	28.0(51.2)	**69.7(81.5)**	
OSH6	25.9(47.3)	27.8(50.0)	23.6(43.6)	28.9(50.5)	28.7(50.1)		
OSH5	26.5(52.8)	24.0(49.2)	24.5(44.0)	**69.7(81.5)**			
OSH4	26.5(52.8)	22.8(46.1)	24.8(48.0)				
OSH3	24.2(45.8)	27.7(49.4)					
OSH2	**55.1(70.9)**						

%IDENTITY (%SIMILARITY)

FIGURE 2.—The identities and similarities between OXYB and the yeast Osh proteins. Percentage identity and similarity (number in parentheses) between the canonical *O.c.* OXYB and its yeast homologues as determined by BESTFIT sequence analysis. The yeast Osh proteins were grouped into four sequence subfamilies on the basis of protein identities exceeding 55% (indicated by highlighted numbers); Osh3p defined its own subfamily and therefore was not >55% identical to another Oshp. Although all Osh proteins shared significant similarity to OXYB over the OSBP domain, the closest identity with OXYB was limited to two subfamilies (corresponding to Osh1p/2p and Osh3p, respectively).

database searches. BLASTP searches identified 39 nonredundant protein homologues from a diverse set of eukaryotes including plants, metazoans, and fungi. Within these proteins, similarity was highest in a small domain of ~150–200 amino acids. The derived consensus sequence for this "OSBP domain" is shown in Figure 1A. Within the OSBP domain, sequence identity was concentrated within three smaller subdomains separated by a region of variable size and sequence unique to each protein (Figure 1A). We defined OSBP homologues by virtue of their similarity to all three subdomains of the OSBP consensus sequence.

The yeast OSBP homologues are encoded by seven "*OSH*" genes: The *S. cerevisiae* genome encoded seven OSBP homologues. These genes corresponded to yeast open reading frames YHR001w, YKR003w, YHR073w, YDL019c, YAR042w, YPL145c, and YOR237w, respectively designated *OSH1–OSH7*.

All yeast *OSH*s encoded proteins with small domains that shared high overall similarity to the OSBP consensus (Figure 1A). Within the OSBP subdomains some residues were invariant in all OSBP homologues. The yeast Osh proteins differed widely in size. The largest proteins, Osh3p, Osh2p, and Osh1p, contained PH domains (Figure 1C) amino-terminal to the OSBP domains (SCHMALIX and BANDLOW 1994; LEVINE and MUNRO 1998). PH domains regulate protein targeting to membranes and thereby serve as membrane adapters (HEMMINGS 1997; LEMMON *et al.* 1997). In addition to PH domains, ankyrin repeats were found within the N-terminal sequences of Osh2p (SCHMALIX and BANDLOW 1994) and Osh1p (Figure 1B). Ankyrin repeats mediate protein-protein interactions and are found in many proteins including cytoskeletal proteins and some transcription factors (reviewed by SEDGWICK and SMERDON 1999). Thus the structure of Osh2p and Osh1p is suggestive of being able to bind both a phosphoinositide lipid through their PH domain and a protein partner through their ankyrin repeats.

If the OSBP domain is responsible for binding oxysterols, it would appear to be a unique sterol-binding motif. By paired BLASTP sequence comparisons, no similarity was found between the OSBP domain and oxysterol-binding steroid nuclear hormone receptors (RUSSELL 1999). In addition, the sterol-binding motif common to SCAP, NPC1, Patched, and HMG-CoA reductase, a motif consisting of five membrane-spanning helices (LANGE and STECK 1998), was not present in any of the OSBP homologues.

On the basis of overall sequence homology the yeast Osh proteins were divided into four subfamily groups: (1) Osh1p and Osh2p, (2) Osh3p, (3) Osh4p and Osh5p, and (4) Osh6p and Osh7p. Over the region of homology, members of each subfamily were at least 55% identical; between subfamilies, identity was <30% (Figure 2). Osh1p, Osh2p, and Osh3p shared greatest homology to OXYB. Like OXYB, these yeast Osh proteins share regions of similarity, such as the PH domain, that lie outside the OSBP consensus domain.

Secondary structure predictions indicated that all yeast Osh proteins are likely to be soluble proteins. Like mammalian OXYB, the yeast Osh proteins lack any predictable membrane-spanning domains. Most hydrophobic spans were too short to traverse a membrane bilayer or were not predicted to be α-helical, and no N-terminal secretory signal sequences were found (Figure 3). Since mammalian OSBP (RIDGWAY *et al.* 1992) and yeast Osh4/Kes1p (FANG *et al.* 1996) have been detected on intracellular membranes, OSBPs are likely to be peripheral rather than integral membrane proteins. Also, like OXYB, potential coiled-coil regions were identified in most of the yeast homologues (Figure 3). On the basis of these secondary structure predictions, OXYB and the yeast Osh proteins were not expected to be integral membrane proteins, but some might bind other membrane proteins through coiled-coil domain interactions. Membrane association may also be conferred by a combination of interactions with membrane proteins, through ankyrin repeats and coiled-coil domains and through lipid/PH domain interactions.

Disruption of the yeast *OSH* genes: To determine whether any of the seven *OSH* genes was necessary for growth, strains in which each *OSH* was deleted and substituted with a prototrophic marker were constructed (see MATERIALS AND METHODS). Haploid cells lacking any single *OSH* gene grew normally regardless of growth medium or temperature. Therefore *OSH*s either were involved in nonessential processes or performed one or more essential but overlapping functions.

Some of the previously characterized *OSH* deletions

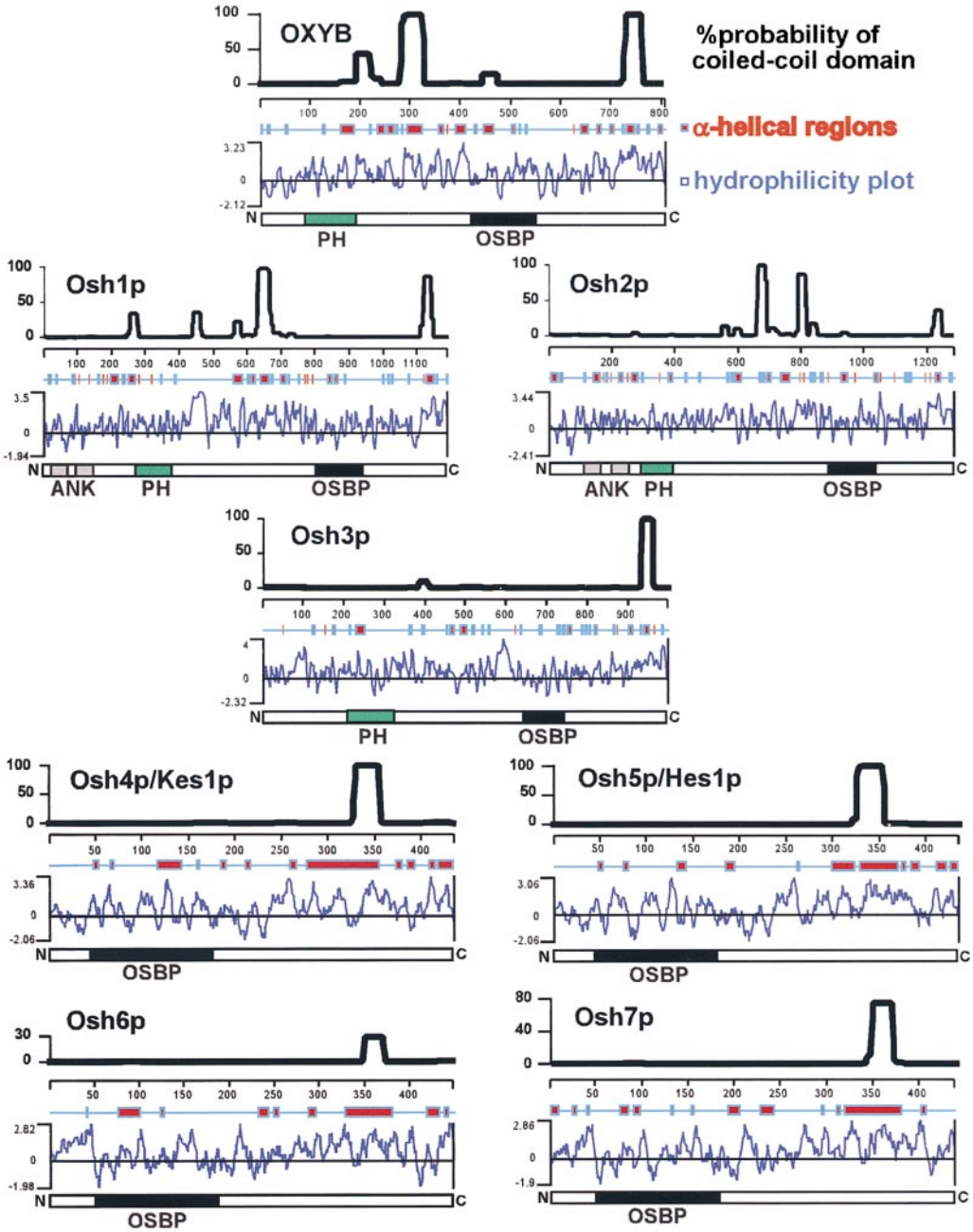

FIGURE 3.—Predicted secondary structure of the yeast Osh proteins. Secondary structure motifs for each yeast Oshp, as well as OXYB, were predicted from their amino acid sequence by three methods. For each protein indicated, the top graph plots the probability of coil-coil domain formation *vs.* amino acid residue number. The second illustration defines blocks of potential α-helical regions. The bottom graph plots hydrophilicity *vs.* residue number. A likely membrane-spanning domain would constitute a contiguous stretch of 19–20 residues predicted to form an α-helix, with a hydrophilicity score of <-1.6 over the entire length (KYTE and DOOLITTLE 1982). By these criteria, none of the OSBPs was likely to be an integral membrane protein. The bottom figure depicts important sequence motifs and their relative positions within each protein. Pleckstrin homology motifs (PH) are indicated by green boxes, ankyrin repeats (ANK) are indicated by shaded boxes, and the OSBP domains (OSBP) are indicated by solid boxes.

had marginal changes in cellular ergosterol concentrations (JIANG *et al.* 1994; FANG *et al.* 1996; DAUM *et al.* 1999). To identify and quantify sterol lipids, saponified lipid extracts from each deletion strain were analyzed by tandem gas chromatography-mass spectroscopy. Relative to extracts from wild type, extracts from most of the deletion mutants had nearly the same level of ergosterol and sterol precursors (Figure 4). Compared to wild type, however, *osh5*Δ and *osh6*Δ strains contained a statistically significant elevation in steady-state ergosterol levels.

Gene expression profiles of the *osh*Δ strains: To determine whether there were any phenotypic differences between each *OSH* deletion mutant, we compared their expression profiles utilizing a collection of promoter-fusion reporter plasmids representing 96 yeast genes (DIMSTER-DENK *et al.* 1999). In each plasmid, a specific gene was fused at the position of the fourth amino acid to the coding region of green fluorescent protein and yeast colonies carrying each individual reporter were independently cultured and assayed for GFP fluorescence. The reporters represented genes encoding all known mevalonate pathway proteins, proteins involved in lipid metabolism, and proteins that respond to other well-established cellular responses (*e.g.*, heat-shock, pheromone induction, and DNA repair; Table 2).

In the analysis of the *OSH* deletion mutants, expression profiles provided a sensitive measure of phenotype, a "fingerprint" of changes in expression in response to

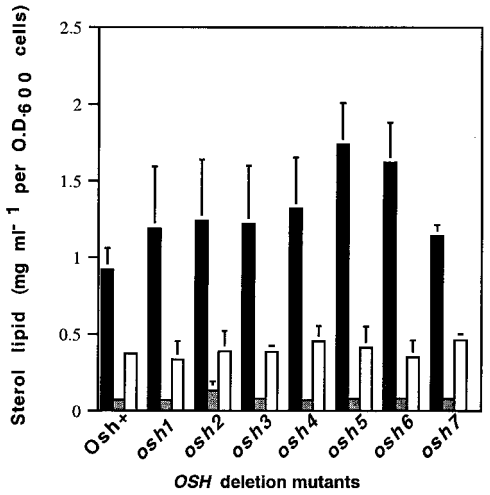

FIGURE 4.—Sterol lipid concentrations of individual *OSH* deletion mutants. From wild type and *OSH* deletion strains, free membrane sterol lipids were extracted and quantified by GC-MS (see MATERIALS AND METHODS). Steady-state amounts of three representative lipids are shown: squalene, lanosterol, and ergosterol. The levels of the other detected sterol lipids were equivalent between wild-type and mutant extracts (our unpublished observations). ■, ergosterol; ▩, lanosterol; □, zymosterol.

the loss of a particular gene. If each of the *OSH*s performed exactly the same cellular function, then the overall expression profiles for each deletion mutant would be identical to each other and to wild type. If the *OSH*s performed different cellular functions, then the profiles for each mutant would be distinct. The expression profiles demonstrated clear differences between deletion mutants and between deletion mutants and wild type (Figure 5). Of the 96 reporter plasmids, 39 were induced or repressed at least twofold in one or more *OSH* deletion mutants (Figure 5). In most cases, the profiles of each *osh*Δ were unique, indicating that the deletion of most *OSH* genes had distinct consequences. The one exception involved *osh5*Δ and *osh6*Δ, whose expression profiles correlated. By this analysis, *OSH5/HES1* and *OSH6* appear to share some functional relatedness, as suggested by the similar sterol lipid composition of *osh5*Δ and *osh6*Δ strains, described above.

The deletion of *OSH4/KES1* appeared to affect expression of the 96 genes to the greatest degree, whereas *OSH2* affected gene expression the least (Figure 5). Several of the genes examined were induced in some *osh*Δ strains but repressed in others (*e.g.*, *ERG8*, *SOD1*). Only a few genes (*COQ1*, *CPS1*, *GSC2*, *SUC2*, YDR516C) were either uniformly repressed or uniformly induced in most *OSH* mutants, and none of these genes function directly in sterol lipid biosynthesis. Only one of these genes, *COQ1*, was involved in isoprenoid biosynthesis (coenzyme Q biosynthesis). If the *OSH* deletions have a common effect on sterol homeostasis, it was not revealed by changes in expression of mevalonate pathway genes.

Bypass suppression of *sec14-1* temperature sensitivity by *OSH* deletion: *SEC14* encodes a phospholipid transfer protein capable of binding both phosphatidylcholine and phosphatidylinositol (BANKAITIS *et al.* 1990). The essential function of *SEC14*, required for secretory export from the Golgi complex, can be bypassed by the deletion of *OSH4/KES1* (FANG *et al.* 1996). To determine if other *OSH* deletions could restore viability to a *SEC14* mutant, each of the seven *osh*Δ strains and their wild-type parent were crossed to a strain (CTY1-1A) bearing the temperature-sensitive allele, *sec14-1*. Diploids were sporulated and tetrads were dissected onto solid rich medium (>15 tetrads analyzed) and incubated at 23°. To test for temperature sensitivity, the dissection plates were replica-printed onto solid rich medium and incubated at 37°. Consistent with previous findings (FANG *et al.* 1996), all *osh4*Δ *sec14-1* spores grew at the restrictive temperature. All spores carrying *sec14-1* and any of the other *OSH* deletions were still temperature sensitive, indicating that the bypass suppression of *sec14* was specific to the *osh4*Δ allele. Moreover, when *osh4*Δ *sec14-1* strains were transformed with high-copy plasmids containing any of the *OSH*s, only the transformant strain with the *OSH4/KES1* plasmid was temperature sensitive. Thus, none of the other *OSH* genes on high-copy-number plasmids could restore *OSH4/KES1* function in the context of the *osh4*Δ suppression of *sec14-1* lethality.

Sterol-related phenotypes of single and multiple *osh*Δ mutants: Inspired by previous studies (JIANG *et al.* 1994) and our finding that some *OSH* deletions affected ergosterol levels, we explored whether all single *osh*Δ mutants manifested sterol-related defects. On rich medium, many sterol-related mutants exhibit a defect in tryptophan transport when grown at low temperatures (GABER *et al.* 1989). Some *osh*Δ strains were reported to grow poorly due to a defect in tryptophan uptake (JIANG *et al.* 1994). In our experiments, however, such growth defects were observed only in mutants with multiple *OSH* deletion alleles (Table 3). We also compared the growth of individual *OSH* mutants (and multiple deletions) to the growth of wild type in the presence of lovastatin, nystatin, or high concentrations of NaCl. All results are catalogued in Table 3 and examples are shown in Figure 6. Lovastatin inhibits HMG-CoA reductase, the rate-limiting step in isoprenoid and sterol lipid biosynthesis (ALBERTS *et al.* 1980) and confers growth sensitivity to strains defective for sterol biosynthesis and its regulation. Nystatin is a polyene antifungal drug that binds directly to ergosterol in the cell membrane (WOODS 1971; WALKER-CAPRIOGLIO *et al.* 1989). Strains resistant to nystatin have reduced levels of ergosterol exposed on the cell surface. Osmotic stress and potential defects in small ion or metabolite transport were examined on 1.2 M NaCl plates. Serial dilutions of each single *OSH* deletion mutant were spotted onto various rich medium plates, and their growth relative to the parental control was recorded (Table 3). Compared to wild type,

TABLE 2

The reporter plasmids tested

GRM plasmid	ORF name	Gene name	Function
1	YPLO28W	*MEV1*	Isoprenoid biosynthesis
2	YML126C	*ERG13*	Isoprenoid biosynthesis
3	YML075C	*HMG1*	Isoprenoid biosynthesis
4	YLR450W	*HMG2*	Isoprenoid biosynthesis
5	YMR208W	*ERG12*	Isoprenoid biosynthesis
6	YMR220W	*ERG8*	Isoprenoid biosynthesis
7	YNR043W	*ERG19*	Isoprenoid biosynthesis
8	YPL117C	*IDI1*	Isoprenoid biosynthesis
9	YJL167w	*ERG20*	Isoprenoid biosynthesis
10	YHR190w	*ERG9*	Isoprenoid biosynthesis
11	YGR175c	*ERG1*	Isoprenoid biosynthesis
12	YHR072w	*ERG7*	Isoprenoid biosynthesis
13	YHR007c	*ERG11*	Isoprenoid biosynthesis
14	YNL280c	*ERG24*	Isoprenoid biosynthesis
15	YML008C	*ERG6*	Isoprenoid biosynthesis
16	YMR202W	*ERG2*	Isoprenoid biosynthesis
17	YLR056W	*ERG3*	Isoprenoid biosynthesis
18	YMR015C	*ERG5*	Isoprenoid biosynthesis
19	YGL012W	*ERG4*	Isoprenoid biosynthesis
20	YBR003w	*COQ1*	Isoprenoid biosynthesis
21	YNR041C	*COQ2*	Isoprenoid biosynthesis
22	YOL096C	*COQ3*	Isoprenoid biosynthesis
23	YGR255c	*COQ6*	Isoprenoid biosynthesis
26	YOR125C	*COQ7*	Isoprenoid biosynthesis
28	YPL172C	*COX10*	Isoprenoid biosynthesis
29	YOR274W	*MOD5*	Isoprenoid biosynthesis
30	YDL090C	*RAM1*	Protein prenylation
31	YKL019w	*RAM2*	Protein prenylation
32	YJR117w	*AFC1*	Protein prenylation
33	YMR274C	*RCE1*	Protein prenylation
34	YDR410C	*STE14*	Protein prenylation
35	YPL069C	*BTS1*	Protein prenylation
36	YGL155W	*CDC43*	Protein prenylation
37	YPR176C	*BET2*	Protein prenylation
38	YJL031c	*BET4*	Protein prenylation
39	YOR370C	*MRS6*	Protein prenylation
40	YCR048w	*ARE1*	Sterol esterification
41	YNR019w	*ARE2*	Sterol esterification
42	YKL182w	*FAS1*	Fatty acid biosynthesis
43	YPL231W	*FAS2*	Fatty acid biosynthesis
44	YNR016c	*ACC1*	Fatty acid biosynthesis
45	YNL130c	*CPT1*	Phospholipid biosynthesis
46	YER026C	*CHO1*	Phospholipid biosynthesis
47	YGR157W	*CHO2*	Phospholipid biosynthesis
48	YJL153c	*INO1*	Inositol biosynthesis
49	YDR452w	*PHM5*	Phosphate metabolism
51	YBR020w	*GAL1*	Galactose metabolism
52	YBR019c	*GAL10*	Galactose metabolism
53	YBR093c	*PHO5*	Phosphate metabolism
54	YJR104c	*SOD1*	Oxidative stress response
55	YHR008c	*SOD2*	Oxidative stress response
56	YCL027w	*FUS1*	Mating cell fusion
57	YNL160W	*YGP1*	Stationary phase response
58	YHR079c	*IRE1*	Unfolded protein response
59	YJL034w	*KAR2*	ER protein chaperone
60	YJL026w	*RNR2*	DNA repair
61	YIL162w	*SUC2*	Carbohydrate metabolism
62	YGR032W	*GSC2*	Carbohydrate metabolism

(*continued*)

TABLE 2

(Continued)

GRM plasmid	ORF name	Gene name	Function
63	YPL116W	*HOS3*	Histone modification
64	YDR461W	*MFA1*	Mating pheromone
65	YML032C	*RAD52*	DNA repair/recombination
66	YOR101w	*RAS1*	cAMP response
67	YAL053w		Unknown membrane protein
68	YAL054c	*ACS1*	Carbohydrate metabolism
69	YJL101c	*GSH1*	Glutathione biosynthesis
70	YJL100w		Unknown
71	YBR094w		Unknown
72	YLR043C	*TRX1*	Thioredoxin system
73	YGR209C	*TRX2*	Thioredoxin system
74	YDL022W	*GPD1*	Carbohydrate metabolism
75	YIL066c	*RNR3*	DNA repair
76	YDR011W	*SNQ2*	Membrane transporter
77	YJL088w	*ARG3*	Amino acid metabolism
78	YCR011c	*ADP1*	Membrane transporter
79	YIL160c	*POT1*	Peroxisomal fatty acid metabolism
80	YDL089W		Unknown
81	YGL013C	*PDR1*	Transcriptional activator
82	YNL129w		Unknown
83	YMR304W	*UBP15*	Possible ubiquitin protease
84	YFL026w	*STE2*	Mating G protein-coupled receptor
85	YCR047c		Possible methyltransferase
86	YNL139c	*RLR1*	Transcription elongation
87	YJL172w	*CPS1*	Nitrogen metabolism
88	YPL111W	*CAR1*	Amino acid metabolism
89	YDR516C		Possible carbohydrate metabolism
90	YHR140w		Unknown membrane protein
91	YHR139C	*SPS100*	Spore wall maturation
92	YGR088W	*CTT1*	Oxidative stress response
93	YNR017w	*TIM23*	Mitochondrial protein translocation
94	YFL014w	*HSP12*	Heat-shock response
95	YFL016c	*MDJ1*	Mitochondrial protein chaperone
96	YIL159w	*BNR1*	Cytokinesis
2641	YDL059C	*RAD59*	DNA repair/meiosis
2643	YDL057W		Unknown
2646	YDL054C		Unknown membrane protein
2647	YDL053C		Unknown

Ninety-six expression reporter plasmids were tested. The plasmid number, open reading frame (ORF) designation, gene name (if applicable), and gene functions are listed. A description of the cloned promoter fragments is presented elsewhere (Dimster-Denk *et al.* 1999).

the *osh1*Δ strain was lovastatin sensitive and somewhat salt sensitive and the *osh2*Δ mutant was nystatin resistant as was the *osh4*Δ strain. Deletion of just *OSH3*, *OSH5/HES1*, or *OSH7* had minimal effects on growth under these conditions. Since three of the deletion mutants had distinguishable phenotypes, these results reaffirmed that the *OSH*s were functionally distinct.

To identify possible genetic interactions among the *OSH*s, crosses were performed to create all combinations of the seven deletion alleles. Of the 127 possible mutant strains ($n = 2^7 - 1$), 122 were viable on tryptophan-supplemented rich medium, 3 were viable only on synthetic medium, and 2 were inviable regardless of growth medium. Viable strains were systematically examined on solid medium for sterol lipid and membrane defects (Figure 6 and Table 3). When compared to wild type, and taking into account growth defects observed on rich medium (containing excess tryptophan), the most common defect noted was lovastatin sensitivity. When incubated with lovastatin at 23°, 30°, or 37°, the growth of 45 mutant combination strains was inhibited 100-fold or more (*e.g.*, Figure 6A). At the temperatures tested, 40 combination strains exhibited a 100-fold or greater resistance to nystatin (*e.g.*, Figure 6B). Although a few strains were resistant to NaCl (Figure 6C), a larger number (19) exhibited a 100-fold or greater sensitivity to NaCl (*e.g.*, Figure 6D). Since many of the strains shared the same nutritional prototrophies,

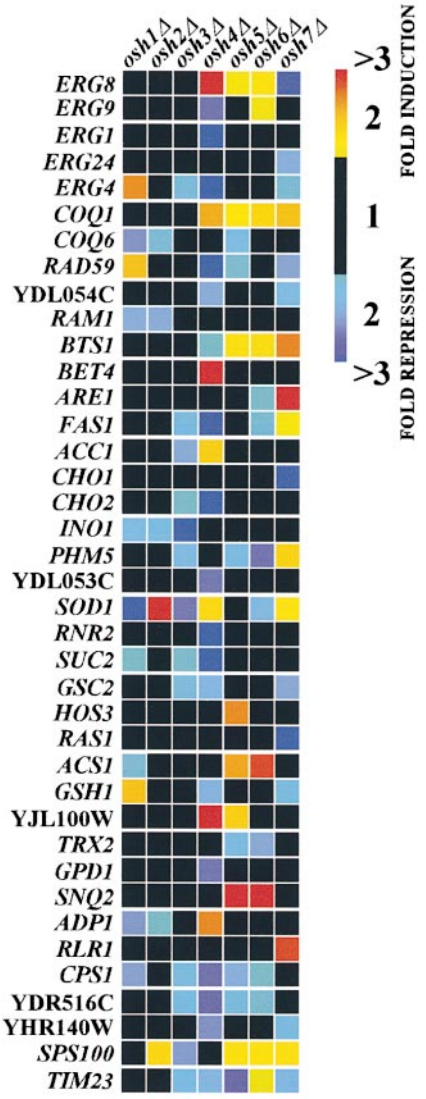

Figure 5.—Expression profile analysis of individual *OSH* deletion mutants. The responses of specific genes to the deletion of individual *OSH*s are represented by color. The magnitude of changes, relative to wild-type controls, is color coded according to the graduation shown. Of the 96 genes listed in Table 2, only the 39 that exhibited a twofold or greater change in expression in at least one mutant profile are displayed. The degrees of correlation between the 21 pairwise comparisons of *OSH* mutant profiles shown are as follows (see MATERIALS AND METHODS): $r(osh6\Delta\&osh7\Delta) = 0.090$ and $t = 0.55$; $r(osh3\Delta\&osh6\Delta) = 0.24$ and $t = 1.52$; $r(osh2\Delta\&osh3\Delta) = -0.15$ and $t = -0.91$; $r(osh1\Delta\&osh2\Delta) = -0.0057$ and $t = -0.034$; $r(osh1\Delta\&osh4\Delta) = -0.11$ and $t = -0.67$; $r(osh4\Delta\&osh5\Delta) = 0.17$ and $t = 1.1$; $r(osh3\Delta\&osh7\Delta) = -0.073$ and $t = -0.45$; $r(osh2\Delta\&osh6\Delta) = 0.018$ and $t = 0.11$; $r(osh1\Delta\&osh3\Delta) = 0.32$ and $t = 2.0$; $r(osh2\Delta\&osh4\Delta) = 0.15$ and $t = 0.93$; $r(osh1\Delta\&osh5\Delta) = 0.048$ and $t = 0.29$; $r(osh2\Delta\&osh7\Delta) = 0.21$ and $t = 1.3$; $r(osh1\Delta\&osh6\Delta) = -0.053$ and $t = -0.32$; $r(osh3\Delta\&osh4\Delta) = 0.11$ and $t = 0.65$; $r(osh2\Delta\&sh5\Delta) = 0.072$ and $t = 0.44$; $r(osh1\Delta\&osh7\Delta) = -0.24$ and $t = -1.5$; $r(osh4\Delta\&osh6\Delta) = 0.11$ and $t = 0.66$; $r(osh3\Delta\&osh5\Delta) = 0.30$ and $t = 1.9$; $r(osh4\Delta\&osh7\Delta) = 0.10$ and $t = 0.61$; $r(osh5\Delta\&osh6\Delta) = 0.91$ and $t = 13.7$; $r(osh5\Delta\&osh7\Delta) = 0.082$ and $t = 0.50$. Only the profiles of *osh5*Δ and *osh6*Δ strains showed statistically significant correlation (at a 99% confidence level).

it was unlikely that marker effects accounted for any of the observed phenotypes. For example, *osh2*Δ *osh3*Δ *osh4*Δ *osh7*Δ and *osh1*Δ *osh3*Δ *osh4*Δ *osh7*Δ shared the same prototrophies but only the latter strain was lovastatin sensitive (Figure 6A). Only a few of the mutants were nystatin sensitive or lovastatin resistant and the effects were relatively small.

Specific effects of deleting various sets of *OSH*s were also evident (Table 3). Under most conditions, mutant combinations that included *osh4*Δ were the most severely affected. For instance, the genotypes of almost all cold-sensitive strains, most salt- or lovastatin-sensitive, and most nystatin-resistant deletion combinations included *osh4*Δ. Under all conditions tested, none of the 11 deletion combinations that grew comparably to wild type included *osh4*Δ. In contrast, 10 of these 11 strains included *osh3*Δ. These results suggested that of the *OSH* family members, deletion of *OSH4/KES1* had the greatest impact on yeast cells and deletion of *OSH3* the least. The genotypes of all salt-resistant strain combinations included *osh6*Δ and/or *osh7*Δ and never included *osh4*Δ. NaCl-sensitive strain combinations were not necessarily sensitive to other salts and many were not osmosensitive. For instance, the strain *osh1*Δ *osh2*Δ *osh3*Δ *osh4*Δ *osh6*Δ was sensitive to 1.2 M NaCl, 0.7 M KCl, 1.0 M sorbitol, and 0.15 M LiCl (Figure 6D). Despite only a minor difference in genotype, the strain *osh1*Δ *osh3*Δ *osh4*Δ *osh5*Δ *osh6*Δ was sensitive only to 1.2 M NaCl. In general, NaCl-sensitive strain combinations that included *osh2*Δ were more likely than others to also be sensitive to 0.7 M KCl. Thus, some deletion combinations caused pleiotropic membrane defects, but others exhibited selective ion sensitivities presumably by disrupting specific ion transport processes. Compared to wild type, mutant strains with larger multiples of *OSH* deletions grew poorly and exhibited both germination defects and extensive flocculation (our unpublished observations). The defects of some *osh*Δ combinations were rescued by additional deletions. For example, the strain *osh1*Δ *osh2*Δ *osh3*Δ was temperature sensitive, lovastatin sensitive, and nystatin resistant but under the same conditions the strain *osh1*Δ *osh2*Δ *osh3*Δ *osh5*Δ grew as well as wild type. Also, the deletion of *OSH1* caused lovastatin sensitivity (at 37°) but in combination with the deletion of *OSH2*, *OSH6*, or *OSH7*, there was no defect. Taken together, these results suggest multiple roles for *OSH* gene family involving sterol lipids and the cell membrane.

Antagonistic interactions between *OSH* genes: In the absence of all the other *OSH*s, strains containing only one of *OSH2*, *OSH3*, *OSH4/KES1*, *OSH6*, or *OSH7* were viable on both rich and synthetic medium (Table 3). In contrast, the strain containing only the *OSH5/HES1* gene was viable on synthetic medium but inviable on rich medium. Spores predicted to have the genotype *osh1*Δ-*4*Δ (Osh5$^+$) *osh6*Δ-7Δ did not germinate on tryptophan-supplemented solid rich medium. They did ger-

TABLE 3

Sterol-related phenotypes of the *OSH* deletion allele combinations

	Rich (+Trp)			Rich Medium			Lovastatin			Nys (5 units)		Nys (20 units)		NaCl		
Deletion genotypes	23°	30°	37°	23°	30°	37°	23°	30°	37°	30°	37°	30°	37°	23°	30°	37°
*osh1*Δ			10S			10S			10^4S							100S
*osh2*Δ												100R				
*osh3*Δ															10R	
*osh4*Δ												1000R	10^4R			
*osh5*Δ												10R	10R			
*osh6*Δ																
*osh7*Δ															10R	
*osh1*Δ*osh2*Δ							10S					10R				
*osh1*Δ*osh3*Δ									10S			10R	10R			
*osh1*Δ*osh4*Δ									1000S			1000R	100R	100S	100S	10S
*osh1*Δ*osh5*Δ									10^4S							10S
*osh1*Δ*osh6*Δ				10S			10S							10R	10R	
*osh1*Δ*osh7*Δ				100S			10S					10R	100R	10R	10R	
*osh2*Δ*osh3*Δ																
*osh2*Δ*osh4*Δ	10S			100S	10S		1000S					1000R	1000R	10S		10S
*osh2*Δ*osh5*Δ												100R				
*osh2*Δ*osh6*Δ												10R	10R		10R	
*osh2*Δ*osh7*Δ												10R	10R	10R	10R	
*osh3*Δ*osh4*Δ							10S									
*osh3*Δ*osh5*Δ																
*osh3*Δ*osh6*Δ													10R			10S
*osh3*Δ*osh7*Δ																
*osh4*Δ*osh5*Δ												100R	10R			
*osh4*Δ*osh6*Δ									10S			100R	100R			
*osh4*Δ*osh7*Δ				1000S	10S		100S					1000R	1000R			
*osh5*Δ*osh6*Δ												10R	10R			
*osh5*Δ*osh7*Δ												100R	1000R	10R		
*osh6*Δ*osh7*Δ												100R	1000R	100R	100R	10R
*osh1*Δ*osh2*Δ*osh3*Δ			100S			100S			100S	10S	100S					10S
*osh1*Δ*osh2*Δ*osh4*Δ			100S			10S			1000S		10S	1000R	100R	10S	10S	100S
*osh1*Δ*osh2*Δ*osh5*Δ												10R	10R			
*osh1*Δ*osh2*Δ*osh6*Δ							10S					10R	10R			
*osh1*Δ*osh2*Δ*osh7*Δ							10S					100R			10R	
*osh1*Δ*osh3*Δ*osh4*Δ							10S		10S					100S	1000S	100S
*osh1*Δ*osh3*Δ*osh5*Δ																

(*continued*)

TABLE 3

(Continued)

Deletion genotypes	Rich (+Trp)			Rich Medium			Lovastatin			Nys (5 units)		Nys (20 units)		NaCl		
	23°	30°	37°	23°	30°	37°	23°	30°	37°	30°	37°	30°	37°	23°	30°	37°
osh1Δosh3Δosh6Δ							10S							10R	10R	
osh1Δosh3Δosh7Δ							100S									
osh1Δosh4Δosh5Δ			100S			10S		10S	10^4S	10S	100S	10R	10R	100S	100S	100S
osh1Δosh4Δosh6Δ			100S			100S			1000S		10S	10R			10S	1000S
osh1Δosh4Δosh7Δ	100S	10S	10S	1000S	10S		1000S	10S	10S		10S		100R	100S	1000S	1000S
osh1Δosh5Δosh6Δ							10S	100S								
osh1Δosh5Δosh7Δ							10S								10R	
osh1Δosh6Δosh7Δ	10S	10S	100S	10S	10S	100S	10S	10S	10^4S	10S	1000S					1000S
osh2Δosh3Δosh4Δ	10S			100S			1000S	100S	10S				100R	100S	1000S	100S
osh2Δosh3Δosh5Δ																
osh2Δosh3Δosh6Δ																
osh2Δosh3Δosh7Δ							10S		1000S					10R		
osh2Δosh4Δosh5Δ									10S			1000R	100R	10S	10S	10S
osh2Δosh4Δosh6Δ								10S	10S			1000R	100R		10S	100S
osh2Δosh4Δosh7Δ				10S		10S	10S		10^4S		10S	10^4R	10R			10^4S
osh2Δosh5Δosh6Δ												10R				
osh2Δosh5Δosh7Δ														10R	10R	
osh2Δosh6Δosh7Δ												1000R	10^4R	10R	10R	
osh3Δosh4Δosh5Δ									10S							
osh3Δosh4Δosh6Δ									100S							
osh3Δosh4Δosh7Δ				10S			100S									
osh3Δosh5Δosh6Δ																
osh3Δosh5Δosh7Δ																
osh3Δosh6Δosh7Δ							100S	10S	10S			10R		10R	10R	
osh4Δosh5Δosh6Δ							10S	100S		10S					10S	10S
osh4Δosh5Δosh7Δ				10S								1000R	100R		10R	
osh4Δosh6Δosh7Δ												10^4R	10^4R	10R	10R	
osh5Δosh6Δosh7Δ												100R	100R	10R		
osh1Δosh2Δosh3Δosh4Δ			10S			10S		100S	10^4S		100S	10R	10R	10S	10S	10S
osh1Δosh2Δosh3Δosh5Δ																
osh1Δosh2Δosh3Δosh6Δ									100S	10S	10S					
osh1Δosh2Δosh3Δosh7Δ							100S	100S	10S							

(*continued*)

TABLE 3

(Continued)

Deletion genotypes	Rich (+Trp)			Rich Medium			Lovastatin			Nys (5 units)		Nys (20 units)		NaCl		
	23°	30°	37°	23°	30°	37°	23°	30°	37°	30°	37°	30°	37°	23°	30°	37°
osh1Δosh2Δosh4Δosh5Δ	10S	10S	100S	10S	10S	100S		100S	10^4S		100S	10R		100S	100S	100S
osh1Δosh2Δosh4Δosh6Δ				10S	10S							1000R	1000R		10S	10S
osh1Δosh2Δosh4Δosh7Δ								10S	100S			1000R	100R			10S
osh1Δosh2Δosh5Δosh6Δ													10R			
osh1Δosh2Δosh5Δosh7Δ						10S			100S							10S
osh1Δosh2Δosh6Δosh7Δ												10R	10R		10R	10R
osh1Δosh3Δosh4Δosh5Δ												10R		10S	10S	10S
osh1Δosh3Δosh4Δosh6Δ								10S	1000S	10S	10S					10S
osh1Δosh3Δosh4Δosh7Δ								1000S	1000S					10S	10S	100S
osh1Δosh3Δosh5Δosh6Δ								10S	1000S	10S						10S
osh1Δosh3Δosh5Δosh7Δ							10S								10R	10R
osh1Δosh3Δosh6Δosh7Δ																
osh1Δosh4Δosh5Δosh6Δ	100S			100S	100S							100R	100R	10S	10S	10S
osh1Δosh4Δosh5Δosh7Δ				10S			100S	10S				10R	10R	10S	10S	100S
osh1Δosh4Δosh6Δosh7Δ	100S			100S			10^4S	100S	1000S			10R	10R	1000S	10^5S	1000S
osh1Δosh5Δosh6Δosh7Δ							100S	100S				10R	10R	10R	100R	10R
osh2Δosh3Δosh4Δosh5Δ	100S			100S				100S	1000S			100R	100R	10S	100S	10S
osh2Δosh3Δosh4Δosh6Δ	1000S			1000S				100S	100S	10S				10S	10S	100S
osh2Δosh3Δosh4Δosh7Δ	100S	10S		1000S	10S		100S	10S	10S	10S	10S	10R	100R	10S	10S	100S
osh2Δosh3Δosh5Δosh6Δ										10S		10R	10R			
osh2Δosh3Δosh5Δosh7Δ			10S			10S				10S	100S					10S
osh2Δosh3Δosh6Δosh7Δ							10S	10S					10R			
osh2Δosh4Δosh5Δosh6Δ				10S	10S							1000R	1000R			10S
osh2Δosh4Δosh5Δosh7Δ												1000R	1000R			10S
osh2Δosh4Δosh6Δosh7Δ	10S			10S		10S	100S		10S	10S	10S	1000R	100R			
osh2Δosh5Δosh6Δosh7Δ												10R	10R		10R	10R
osh3Δosh4Δosh5Δosh6Δ									10S				10R			
osh3Δosh4Δosh5Δosh7Δ								1000S	1000S	10S	10S					
osh3Δosh4Δosh6Δosh7Δ								10S	100S		10S			10S	10S	10S
osh3Δosh5Δosh6Δosh7Δ														10R		
osh4Δosh5Δosh6Δosh7Δ							100S	1000S				10R	100R		10R	
osh1Δosh2Δosh3Δosh4Δosh5Δ	10S	10S		10S	10S			100S	1000S		10S	100R	10R	100S	100S	100S
osh1Δosh2Δosh3Δosh4Δosh6Δ	10S	10S		10S	10S			10S	1000S		10S			100S	10^5S	100S
osh1Δosh2Δosh3Δosh4Δosh7Δ	*															
osh1Δosh2Δosh3Δosh5Δosh6Δ								10S	1000S							10S

(*continued*)

TABLE 3

(Continued)

Deletion genotypes	Rich (+Trp)			Rich Medium			Lovastatin			Nys (5 units)		Nys (20 units)		NaCl		
	23°	30°	37°	23°	30°	37°	23°	30°	37°	30°	37°	30°	37°	23°	30°	37°
osh1Δosh2Δosh3Δosh5Δosh7Δ									10S					10R		
osh1Δosh2Δosh3Δosh6Δosh7Δ			10S			10S		100S	1000S	10S	100S			10R		10S
osh1Δosh2Δosh4Δosh5Δosh6Δ	10S			10S	10S			10S	100S			10R	10R	10S	10S	10S
osh1Δosh2Δosh4Δosh5Δosh7Δ												10^5R	1000R	10R		
osh1Δosh2Δosh4Δosh6Δosh7Δ	*															
osh1Δosh2Δosh5Δosh6Δosh7Δ												100R	100R	10R	10R	10R
osh1Δosh3Δosh4Δosh5Δosh6Δ									10S					100S	100S	10S
osh1Δosh3Δosh4Δosh5Δosh7Δ	100S			1000S	100S		100S	10S	10S	10S	10S			10S	10S	10S
osh1Δosh3Δosh4Δosh6Δosh7Δ												10R	10R	10R		10R
osh1Δosh3Δosh5Δosh6Δosh7Δ							100S	100S	1000S					10R	10R	10R
osh1Δosh4Δosh5Δosh6Δosh7Δ	10S	10S		1000S	100S				10S			100R	100R	10S	10S	10S
osh2Δosh3Δosh4Δosh5Δosh6Δ	1000S	10S		1000S	10S		10S	100S	100S					100S	100S	100S
osh2Δosh3Δosh4Δosh5Δosh7Δ	1000S	1000S	1000S	1000S	100S	1000S	10S	100S	1000S	10^4S	1000S			100S	100S	100S
osh2Δosh3Δosh4Δosh6Δosh7Δ									10S			100R	10R	10R		10S
osh2Δosh3Δosh5Δosh6Δosh7Δ									1000S					10R		
osh2Δosh4Δosh5Δosh6Δosh7Δ					10S							10^4R	100R	10R		
osh3Δosh4Δosh5Δosh6Δosh7Δ							100S	1000S	10^4S							
osh1Δosh2Δosh3Δosh4Δosh5Δosh6Δ	100S	10S		1000S	100S		100S	100S	1000S	100S	10S			100S	100S	1000S
osh1Δosh2Δosh3Δosh4Δosh5Δosh7Δ	10S	10S	100S	1000S	10S	100S	100S	10S	1000S	100S	1000S			100S	100S	1000S
osh1Δosh2Δosh3Δosh4Δosh6Δosh7Δ	*															
osh1Δosh2Δosh3Δosh5Δosh6Δosh7Δ							10S	10S	100S					10R	10R	10R
osh1Δosh2Δosh4Δosh5Δosh6Δosh7Δ	100S	100S	100S	1000S	100S	100S	100S	100S	100S	100S	100S			100S	100S	100S
osh1Δosh3Δosh4Δosh5Δosh6Δosh7Δ	100S			1000S	100S		100S	1000S	10^4S					10S	10S	10S
*osh2Δosh3Δosh4Δosh5Δosh6Δosh7Δ osh*Δ																

All viable *OSH* deletion combinations were tested for sterol-related phenotypes. The table quantitatively summarizes the defects observed on rich solid medium where 10-fold serial dilutions of each mutant strain and their wild-type parent (SEY6210) were spotted. In 10-fold increments, S denotes the magnitude of sensitivity to the conditions tested and R the resistance of the deletion mutants as compared to wild-type growth. Concentrations of additives (in rich medium) are as follows: 50 mg/liter tryptophan; 150 μg/ml lovastatin; 5 units/ml nystatin; 20 units/ml nystatin; 1.2 M NaCl; 0.7 M KCl; 1.0 M sorbitol; 0.15 M LiCl. Media containing nystatin, lovastatin, sorbitol, or any salt were also supplemented with 50 mg/liter tryptophan. At 23°, the wild-type strain grew poorly or not at all in the presence of 5 or 20 units/ml (unlike many of the deletion strains) and therefore was not useful for quantitative comparison. On rich medium, with or without tryptophan, and on sorbitol, 5 units/ml nystatin, LiCl, or KCl-containing medium, the strains were incubated for 1, 1–2, and 2 days at 37°, 30°, and 23°, respectively. All strains were incubated in the presence of 20 units/ml nystatin and lovastatin for 2, 3, and 4 days at 37°, 30°, and 23°, respectively. To determine relative resistance to 1.2 M NaCl, strains were examined after 2, 3, and 4 days at 37°, 30°, and 23°, respectively. To record sensitivities to 1.2 M NaCl, strains were examined after 3, 5, and 7 days at 37°, 30°, and 23°, respectively. To record 1.2 M NaCl resistance, all strains were examined after 2, 3, and 5 days at 37°, 30°, and 23°, respectively. Resistance to nystatin was recorded only as a function of high concentrations (20 units/ml nystatin), and sensitivity was recorded only for low concentrations (5 units/ml nystatin). Strains that grew on minimal medium but did not grow on rich medium are indicated with an asterisk (*). The last two strains listed represent lethal combinations of deletions.

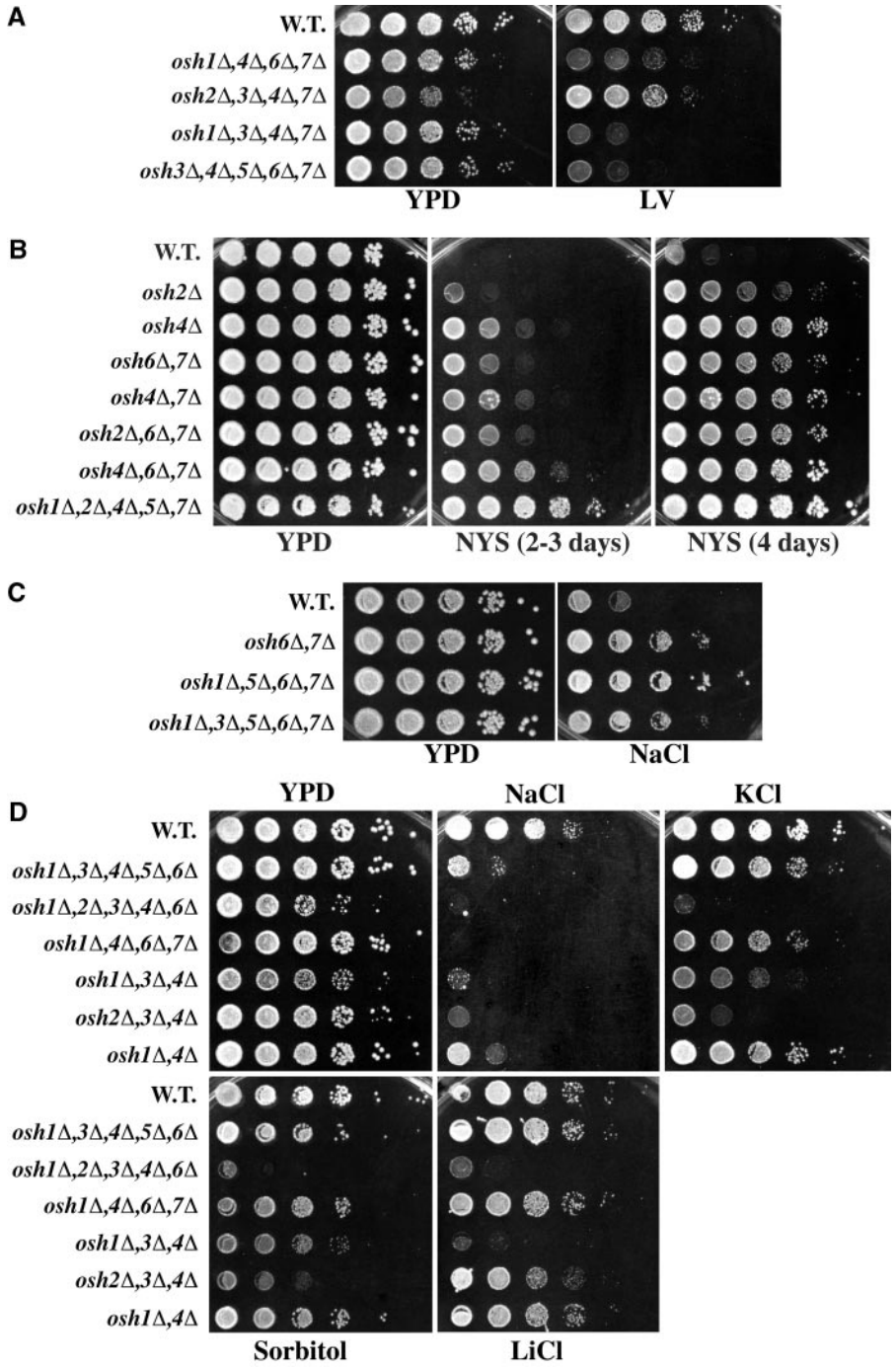

FIGURE 6.—Sterol-related *OSH* mutant phenotypes. Tenfold serial dilutions of wild type and various *OSH* deletion mutants were spotted onto rich medium and onto rich medium containing (A) 150 μg/ml lovastatin, (B) 20 units/ml nystatin, (C) 1.2 M NaCl, and (D) 1.2 M NaCl, 0.7 M KCl, 1.0 M sorbitol, and 0.15 M LiCl. All plates were supplemented with excess tryptophan (see MATERIALS AND METHODS) and incubated at 30°. The strains were incubated for the times described in Table 3 and then photographed.

minate on synthetic medium, but were inviable when streaked onto solid rich medium (Figure 7). Strains containing both *OSH1* and *OSH5/HES1*, in the absence of the other *OSH* genes, were viable on all media tested (Figure 7). As shown below, without other *OSH*s, *OSH1* was itself insufficient to maintain viability on rich or on synthetic medium. The *OSH1* gene seemed to augment the functions of *OSH5/HES1* such that together the genes could impart growth on both types of media when the other *OSH* genes were disrupted.

Remarkably, some genetic interactions between the *OSH*s were antagonistic. Most dramatically, the lethality of some specific deletion combinations on rich medium was suppressed by deletion of an additional gene. Spores containing *OSH5/HES1* and *OSH6* or *OSH3* and *OSH5/HES1* as the only *OSH* genes germinated only on synthetic medium and did not grow when streaked onto solid rich medium (Figure 7). However, when *OSH5/HES1* was disrupted in these strains, growth (albeit poor) was restored on both rich and synthetic media (Figure 7) and spores containing only *OSH3* or *OSH6* germinated on rich medium. Thus *OSH5/HES1* was functionally antagonistic to *OSH3* and *OSH6* in cells grown on rich medium.

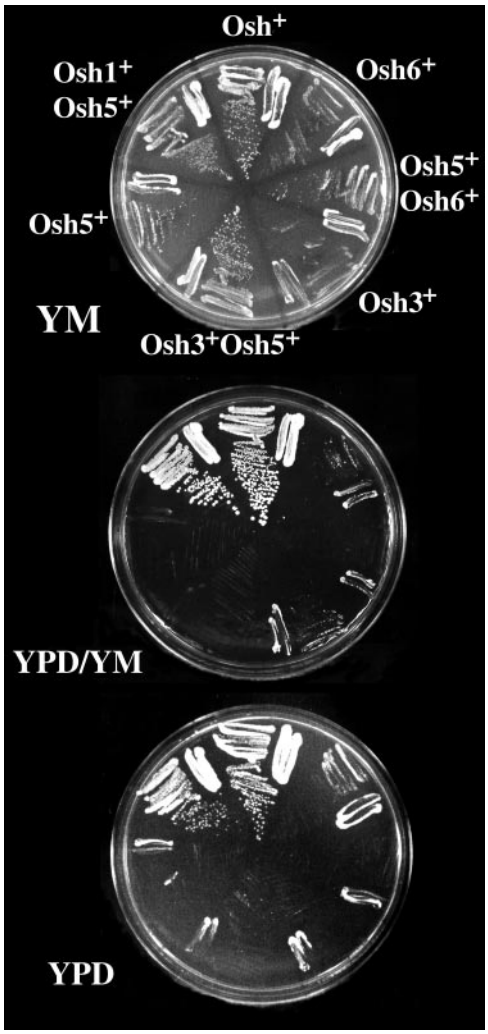

FIGURE 7.—Media sensitivities of the *OSH* deletion combinations. Specific *OSH* deletion strains could be propagated on YM synthetic medium but were unable to grow on YPD rich medium or on solid medium containing a mixture of both YM and YPD. Wild-type (Osh$^+$) (SEY6210), *osh1*Δ-*5*Δ (Osh6$^+$) *osh7*Δ (JRY6324), *osh1*Δ-*4*Δ (Osh5$^+$ and Osh6$^+$) *osh7*Δ (JRY6308), *osh1*Δ-*2*Δ(Osh3$^+$)*4*Δ-*7*Δ (JRY6323), *osh1*Δ-*2*Δ (Osh3$^+$) *osh4*Δ (Osh5$^+$) *osh6*Δ-*7*Δ (JRY6304), *osh1*Δ-*4*Δ (Osh5$^+$) *osh6*Δ-*7*Δ (JRY6319), and (Osh1$^+$) *osh2*Δ-*4*Δ (Osh5$^+$) *osh6*Δ-*7*Δ (JRY6299) were streaked onto YM synthetic, YPD/YM mixed, and YPD rich media. The strains grew at 30° for 3 days before they were photographed.

Media mixing experiments were also conducted to better determine the medium component limiting the growth of these "media-sensitive" strains. *OSH* deletion strains were streaked onto a solid mixture of rich and synthetic media and onto each individual constituent medium. To ensure that tryptophan was not limiting, excess tryptophan was added to all media (see MATERIALS AND METHODS). All strains unable to grow on rich medium, but viable on synthetic medium, were also unable to grow on the mixed medium (Figure 7). Since both the mixed and synthetic media shared the same pH (5.5), and these strains grew only on synthetic medium,

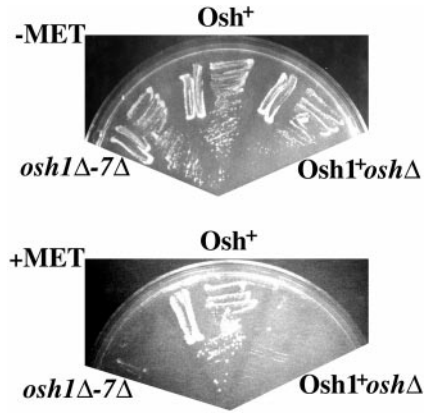

FIGURE 8.—Lethal *OSH* deletion allele combinations. Two of the *OSH* deletion combinations were inviable regardless of growth medium. Strains including wild type (Osh$^+$) (SEY6210), P^{MET3}-*OSH2 osh1*Δ-*7*Δ (JRY6326), and P^{MET3}-*OSH2* (Osh1$^+$) *osh2*Δ-*osh7*Δ (JRY6321) were streaked onto synthetic solid medium without (−Met) or with (+Met) added methionine. Plates were photographed after incubation for 4 days at 30°.

growth was not restricted by pH differences. These results indicated that rich medium contained an inhibitor to the growth of these strains.

The yeast *OSH* genes shared at least one common essential function: Although each *OSH* gene was dispensable for viability, together the *OSH*s defined an essential gene family. In crosses with each *OSH* deletion marked with a prototrophic marker, spores lacking all seven genes could not be isolated, regardless of growth medium. To evaluate independently the effect of deleting all *OSH*s, an integrated P^{MET3}-*OSH2* construct was used to suppress *osh1*Δ-*7*Δ strain inviability. When the *OSH2* gene was expressed, the *osh1*Δ-*7*Δ P^{MET3}-*OSH2* strain (JRY6326) was viable. In the presence of added methionine, however, expression of *OSH2* was repressed and the strain failed to grow (Figure 8). If *osh1*Δ-*7*Δ P^{MET3}-*OSH2* cells were grown for 24 hr in methionine-containing medium and micromanipulated onto solid medium lacking methionine, 75% (36 out of 48) recovered the growth arrest and formed colonies (96% of wild-type cells formed colonies under the same conditions). Thus, the inviability of most *osh1*Δ-*7*Δ cells could be reversed if *OSH2* expression was reactivated after growth arrest. These results confirmed the essential requirement of yeast for the *OSH*s.

Although only two individual deletions of *OSH* genes even modestly affected sterol lipid levels, we examined whether depletion of all Osh proteins from yeast would have a greater effect. To deplete yeast of Osh proteins, methionine was added to exponentially growing *osh1*Δ-*7*Δ P^{MET3}-*OSH2* cells. Following growth arrest (corresponding to about four culture doublings), lipids were extracted, saponified, and quantified. Analysis of the extracted sterol lipids by GC-MS indicated a severe perturbation of normal sterol levels. For example, ergo-

TABLE 4

Sterol lipid levels after Osh1p-7p depletion

Sterol lipid	Wild-type cells lipid amount (μg/mg protein)	Osh1p-7p depleted cells	
		Lipid amount (μg/mg protein)	Fold change relative to wild type
Ergosterol	67.8 ± 10.3	237 ± 34.8	3.5
Zymosterol	10.4 ± 2.7	31.0 ± 3.9	3.0
Episterol[a]	6.2 ± 3.4	8.1 ± 2.0	1.3
22-Dihydroergosterol	5.6 ± 2.7	70.3 ± 14.7	13
Fungisterol[a]	4.1 ± 0.8	8.2 ± 2.0	2.0
Fecosterol	4.0 ± 2.1	11.3 ± 1.4	2.9
Lanosterol	3.8 ± 2.5	6.8 ± 0.4	1.8

[a] Identities of episterol and fungisterol were assigned solely on basis of molecular weight.

sterol concentrations increased 3.5-fold, and 22-dihydroergosterol levels increased 13-fold relative to wild type and, by varying degrees, there were steady-state increases in the levels of many other sterols (Table 4). Some sterol lipids remained largely unaffected by Oshp depletion (*e.g.*, episterol). These results were also consistent with observations by microscopy using the fluorescent sterol-binding polyene, filipin. Fixed cells depleted of Osh proteins and treated with filipin appeared to have significantly greater filipin/sterol fluorescence (our unpublished observations). These results established that an important function of all *OSH*s, perhaps their essential function, is the maintenance of cellular sterol lipid composition.

Of all seven *OSH* genes, only *OSH1* was incapable of maintaining viability in the absence of the other genes, regardless of growth medium. In crosses with marked *OSH* deletions, spores in which *OSH1* was the only *OSH* gene left intact could not be isolated. An (Osh1$^+$) *osh2*Δ-7Δ P^{MET3}-*OSH2* strain could be propagated in the absence of methionine but not in its presence (Figure 8). However, multicopy plasmids containing any of the *OSH* genes, including *OSH1* itself, were able to support growth of the *osh1*Δ-7Δ P^{MET3}-*OSH2* strain on a medium repressing *OSH2* expression (our unpublished observations). Thus, each of the seven *OSH* genes, including *OSH1* if overexpressed, had the capacity to maintain the essential function(s) common to all yeast Osh proteins.

DISCUSSION

This study provided a comprehensive evaluation of the gene family defined by its homology to the mammalian *OXYB* oxysterol-binding protein. Although this family is present in all eukaryotes examined, the *in vivo* role of these proteins is unclear. Homozygous OXYB knockout mice fail to develop beyond the first zygotic divisions (J. Goldstein, personal communication) indicating that the protein carries out an essential function.

Each *OSH* performed a specific and unique function: In yeast, null alleles of any single *OSH* gene had no discernible effect on growth on standard media. However, using broad-based assays guided by the biochemical clue that the family may have a role in sterol metabolism, clear phenotypes were found for the *OSH* genes. The phenotypes of *osh* deletion mutants allowed some functions of the yeast Osh proteins to be deduced. First, three single deletion mutations caused cells to be resistant to nystatin, a polyene antibiotic whose toxicity to yeast is proportional to the amount of ergosterol in the cell membrane. Although *osh2*Δ and *osh4*Δ mutants were resistant to nystatin, they contained wild-type levels of ergosterol. This result suggested that less ergosterol was exposed at the cell membrane in these mutants and, since total ergosterol levels were the same as wild type, some resided at other locations shielded within the cell. Thus, *OSH2* and *OSH4/KES1* may facilitate the transfer of ergosterol to the cell membrane. In contrast, *osh1*Δ strains were sensitive to lovastatin, an inhibitor of an early step in sterol biosynthesis, yet had wild-type levels of sterol lipids. Therefore, *osh1*Δ strains had no defect in sterol biosynthesis *per se*, but the lovastatin sensitivity indicated a defect in the postsynthetic regulation of sterol lipid function. Indeed *osh5*Δ and *osh6*Δ mutants had elevated sterol levels. Thus, at some level *OSH1*, *OSH5/HES1*, and *OSH6* were required for the proper regulation of sterol biosynthesis.

As a second and independent evaluation of the relationships among the *OSH* genes, we compared the expression profiles of 96 genes selected to include genes involved in all aspects of sterol biosynthesis and a range of other processes. This analysis was not based on any assumption about Osh proteins being regulators of transcription. Rather, transcription of the selected genes was simply used as a broad-based molecular phenotype. This analysis revealed clear and distinct differences between all *OSH* mutants and wild type. With one exception, the pattern of each mutant expression profile was distinctly different from the other mutants, indicating that each *OSH* had a specific role. The most similar

expression profiles were those of *osh5*Δ and *osh6*Δ, which were the only two mutations that individually affected sterol levels.

The use of expression profiles and subtle phenotypes allowed us to dismiss a conventional interpretation of mutants that have little or no phenotype. Specifically, when individual members of a gene family are disrupted and have no readily discernible phenotypic consequences, functional redundancy is often offered as an explanation. As shown here, by expanding the range of phenotypes examined, there was no difficulty establishing that every family member executed a unique function in the cell. Thus, by definition, these genes were not functionally redundant. This analysis did not exclude the possibility that each member of the gene family carried out a common function and, as discussed below, that was exactly the case for the *OSH* genes.

The *OSH* family members each performed a common essential function: The phenotypes of all 127 possible combinations of *OSH* mutants revealed some simple conclusions and a wealth of phenotypic complexity. To emphasize the most salient result, the lack of all seven *OSH* genes caused growth arrest. In cells without *OSH* genes, growth could be restored by any one *OSH* gene on a multicopy plasmid. Thus, the seven yeast *OSH* genes, which together shared only a small region of sequence identity, shared at least one essential overlapping function. At face value, it seems incongruent that the knockout of a single OSBP gene in mouse was lethal, but the deletion of all *OSH* genes was required to kill a yeast cell. A simple explanation might be that the mouse ovum does not carry a maternal store of OSBPs and OXYB is the only OSBP expressed during the early stages of development.

The regulated expression of a single *OSH* gene in a strain lacking all seven chromosomal copies of *OSH* genes allowed us to grow these cells and determine what happens when the last remaining *OSH* gene is shut off. The most striking result was a 3.5-fold increase in the total level of ergosterol in the cell, a dramatic enhancement over the modest increases observed in the *osh5*Δ and *osh6*Δ single mutants. This induction is astonishing in comparison to wild-type levels of ergosterol, which are normally present at 3.3-fold molar excess over all plasma membrane phospholipids (Zinser *et al.* 1991). How the yeast cell accommodates the elevation of ergosterol levels to 3.5-fold above normal is a challenge to conventional models of membrane organization. Either the cell membrane adapts to the increased level of ergosterol, perhaps through compensatory changes in other lipid concentrations, or the excess ergosterol accumulates within the cell.

Because the high level of ergosterol overproduction was observed only when the entire *OSH* family was deleted, each single gene could prevent the massive overproduction of ergosterol and hence each *OSH* had a common regulatory role. It was unclear, however, whether this ergosterol regulatory role was a direct or indirect part of the common essential function shared by all *OSH*s.

Lessons from combinations of *OSH* genes: The phenotypes of all mutant combinations are described in Table 3, but certain phenotypes warrant particular attention. First, although the primary structures of the seven *OSH*s fall into four subfamilies, there was little evidence that phenotypes were apt to be more similar among mutants representing the same sequence subfamily. For example, *OSH4/KES1* and *OSH5/HES1* define a subfamily, yet the deletion of *OSH4/KES1*, but not *OSH5/HES1*, had appreciable impacts on growth, salt and lovastatin sensitivity, and nystatin resistance. Second, although most *OSH*s shared a common essential function, deletion of particular *OSH* genes often had completely different consequences in viable deletion strains. For example, in contrast to *OSH4/KES1* deletion mutants, most of which were NaCl sensitive, all NaCl-resistant strains lacked *OSH6* or *OSH7*.

The NaCl sensitivity of many *OSH* deletion strains indicated that the yeast Osh proteins affected the cell membrane in several different ways. Some of these strains were sensitive to other salts and conditions that affect cellular osmolarity. Some of the other strains were sensitive to NaCl and only to other specific salts, indicating ion-specific sensitivities. The results suggest that certain deletion combinations generally affect membrane permeability, while others specifically affect ion transport.

Even more surprising was evidence that some *OSH*s work at cross purposes. This conclusion was based in part on an unanticipated dependence of certain mutant combinations on a particular medium to grow. Specifically, certain mutant combinations grew on synthetic medium but not on rich medium, a phenomenon we currently do not understand. However, clearly rich medium contained an inhibitory substance. Some pairs of *OSH* genes (*OSH5/HES1* and *OSH6*; or *OSH3* and *OSH5/HES1*) supported growth on minimal medium but not on rich medium, whereas *OSH3* or *OSH6* alone supported growth on both media. Thus, some individual *OSH* genes are better than two. Similarly, based upon other phenotypes, cells containing only *OSH4/KES1*, *OSH6*, and *OSH7* grew better than cells containing only *OSH4/KES1*, *OSH5/HES1*, *OSH6*, and *OSH7*. In both of these cases, the presence of *OSH5/HES1* seemed to antagonize the function of the other *OSH*s.

Although unusual, the ability of smaller subsets of a gene family to be better for a cell than larger subsets has been seen before in the case of kinesins. Kinesins are microtubule motors that have a characteristic polarity and can move toward only one end of a microtubule. Plus-end movement requires one class of motors and minus-end movement requires a different class of motors (reviewed in Hildebrandt and Hoyt 2000). Cells lacking too many kinesins of a particular class grow

poorly or die, but viability can be restored either by adding back the missing motors or by removing a subset of the motors of the other class (Saunders and Hoyt 1992; Hoyt *et al.* 1993). Apparently, a balance of motor types is more critical for cells than the presence or absence of any particular kinesin. If this principle applies to *OSH* genes, in some contexts the *OSH5/HES1* gene would appear to carry out a process in opposition to *OSH3* or *OSH6*. The direction of lipid transport could underlie this phenomenon.

The structure of OSBPs: The function of the defining motif of the OSBP protein family, the 150-amino-acid tripartite consensus, remains unknown. Although the OXYB protein binds oxygenated sterols directly, it is not clear whether binding is mediated by this conserved motif or by an adjacent region. OSBP family members lack any apparent transmembrane domains, but may function at the surface of membranes. Indeed the Osh1p, Osh4p, and the mammalian OXYB protein associate with vesicle and Golgi membranes (Ridgway *et al.* 1992; Fang *et al.* 1996; Levine and Munro 1998). Although the intracellular localization of Osh2p and Osh3p is unknown, they have a PH domain like Osh1p. Moreover, the PH domain of Osh1p binds phosphatidylinositol lipids (Levine and Munro 1998) suggesting that Osh2p and Osh3p may also bind membranes and specifically interact with phosphatidylinositol. Ankyrin repeats, motifs that mediate protein-protein interactions (Sedgwick and Smerdon 1999), found in some of the Osh proteins, and the coiled-coil domains found in all of them, certainly invite the notion that they are a part of larger protein complexes.

Prokaryotes lack sterols and their genomes lack genes encoding OSBPs. OSBP homologues have been found in all eukaryotic genomes examined, including organisms such as *Drosophila melanogaster* and *Caenorhabditis elegans*, which have lost the ability to synthesize sterols. *C. elegans* contains four OSBP homologues and Drosophila contains three (*C. elegans* Sequencing Consortium 1998; Adams *et al.* 2000). In both these cases, the total number of OSBPs is fewer than found in genomes of eukaryotes that can synthesize sterols (*e.g.*, *S. cerevisiae*, *Arabidopsis thalius*, *Homo sapiens*). Clearly, the selection to keep these genes seems independent of sterol biosynthesis. Moreover, as in OSBPs from sterol prototrophs, PH domains and coiled-coil regions were found in some of the *C. elegans* and Drosophila homologues (C32F10.1, Y47D3A.17 and Cg1513, *D.m.* OSBP, respectively). Structural motifs present only in *C. elegans* or Drosophila OSBPs could not be found. [To date only yeasts, namely *S. cerevisiae* and *Schizosaccharomyces pombe*, have OSBP homologues with ankyrin repeats (*OSH1*, *OSH2* and SPBC2F12.05c, respectively)]. However, regardless of species, sterol lipids in all eukaryotes must be transported to the membranes where they are needed, a process in which OSBP homologues may play an integral part.

A role of an *OSH* in vesicular trafficking: A firm link between a yeast *OSH* and membrane transport was established through the analysis of the *SEC14*-encoded phosphatidylcholine/phosphatidylinositol transfer protein (Fang *et al.* 1996). Cells lacking this protein are inviable due to the inability of transport vesicles to bud from the Golgi apparatus. Mutations in *OSH4/KES1*, *SAC1*, or mutations in any of several genes involved in phosphatidylcholine synthesis restore viability to *SEC14* mutants (reviewed by Xinmin *et al.* 2000). We extended earlier observations (Fang *et al.* 1996) and determined that *OSH4/KES1* was the only *OSH* gene in which mutations restore viability to *SEC14* mutants.

Although the mechanism by which *osh4/kes1* mutations bypass the *SEC14* requirement is unknown, it has been suggested that the other *sec14* bypass suppressors alter the lipid composition of the Golgi membrane (Xinmin *et al.* 2000). Presumably the Sec14p PI/PC lipid transport protein maintains a Golgi membrane that is competent to support vesicle budding, and this competence is lost in *SEC14* mutants. Presumably the suppressors reestablish Golgi membrane budding by restoring a favorable lipid composition. A simple model that explains how *OSH4/KES1* mutants are *sec14* suppressors would be that loss of *OSH4/KES1* leads to a budding-competent Golgi membrane. This implies that the normal function of *OSH4/KES1* is to prevent inappropriate vesicle formation by creating an unfavorable lipid composition. Vesicle biogenesis would therefore require the proper balance between Sec14p and Osh4p to create a membrane competent for budding from the Golgi.

If Osh4p changes Golgi lipid composition, it does not do so by altering total cellular levels of ergosterol or phosphatidylcholine. Total levels of sterol lipids were normal in the *osh4*Δ strain (Figure 4; Fang *et al.* 1996) and deletion of *OSH4/KES1* does not reduce flux through the CDP-choline pathway (Fang *et al.* 1996). Overexpression of *OSH4/KES1* on multicopy plasmids also abrogates the suppression of the *sec14* defect by phosphatidylcholine synthesis mutants (Fang *et al.* 1996). Thus, Osh4p function is independent of phosphatidylcholine synthesis and changes to the levels of any other lipids would appear to be restricted to the Golgi.

Vesicular transport is a cornerstone of secretion, so it is worth considering whether the function of *SEC14* and *OSH4/KES1* in the Golgi extends to other aspects of secretory transport. Recently four structural homologues of *SEC14* have been characterized in yeast and, under the appropriate conditions, have been shown capable of carrying out the role of *SEC14* (Li *et al.* 2000). Perhaps the principal role of these *SEC14* homologues is to promote vesicle formation from membranes other than the Golgi. Other Osh proteins may serve with these proteins to perform a role similar to that of Osh4p with Sec14p. If the yeast OSBP family regulates budding from many different membrane compartments, then we

would predict that cells lacking Osh proteins would accumulate a variety of vesicles or aberrant organelles.

Special thanks to Howard Bussey for strains and to Nancy Hawkins for her critical reading of the manuscript. We thank Stewart Scherer for comments and discussion and Sean Munro, Howard Bussey, and Vitas Bankaitis for advice on achieving a common *OSH* nomenclature. This work was funded by a National Institutes of Health grant to J.R. (GM35827). C.T.B. was supported by an American Cancer Society postdoctoral fellowship and a Leukemia and Lymphoma Special Fellows grant.

LITERATURE CITED

Adams, A., D. E. Gottschling, C. A. Kaiser and T. Stearns, 1997 *Methods in Yeast Genetics*. Cold Spring Harbor Laboratory Press, Cold Spring Harbor, NY.

Adams, M. D., S. E. Celniker, R. A. Holt, C. A. Evans, J. D. Gocayne *et al.*, 2000 The genome sequence of *Drosophila melanogaster*. Science **287:** 2185–2195.

Alberts, A. W., J. Chen, G. Kuron, V. Hunt, J. Huff *et al.*, 1980 Mevinolin: a highly potent competitive inhibitor of hydroxymethyl glutaryl-coenzyme A reductase and a cholesterol lowering agent. Proc. Natl. Acad. Sci. USA **77:** 3957–3961.

Alphey, L., J. Jimenez and D. Glover, 1998 A Drosophila homologue of oxysterol binding protein (OSBP)—implications for the role of OSBP. Biochim. Biophys. Acta **1395:** 159–164.

Altschul, S. F., W. Gish, W. Miller, E. W. Myers and D. J. Lipman, 1990 Basic local alignment sequence tool. J. Mol. Biol. **215:** 403–410.

Bankaitis, V. A., D. E. Malehorn, S. D. Emr and R. Greene, 1989 The Saccharomyces cerevisiae *SEC14* gene encodes a cytosolic factor that is required for transport of secretory proteins from the yeast Golgi complex. J. Cell Biol. **108:** 1271–1281.

Bankaitis, V. A., J. R. Aitken, A. E. Cleves and W. Dowhan, 1990 An essential role for a phospholipid transfer protein in yeast Golgi function. Nature **347:** 561–562.

Bard, M., R. A. Woods, D. H. Barton, J. E. Corrie and D. A. Widdowson, 1977 Sterol mutants of Saccharomyces cerevisiae: chromatographic analyses. Lipids **12:** 645–654.

Barnes, G., and J. Thorner, 1986 Genetic manipulation of *Saccharomyces cerevisiae* by use of the *LYS2* gene. Mol. Cell. Biol. **6:** 2828.

Boeke, J. D., F. LaCroute and G. R. Fink, 1984 A positive selection for mutants lacking orotidine-5′-phosphate decarboxylase activity in yeast: 5-fluoro-orotic acid resistance. Mol. Gen. Genet. **197:** 345.

Brown, M. S., and J. L. Goldstein, 1997 The SREBP pathway: regulation of cholesterol metabolism by proteolysis of a membrane-bound transcription factor. Cell **89:** 331–340.

Brown, M. S., and J. L. Goldstein, 1999 A proteolytic pathway that controls the cholesterol content of membranes, cells, and blood. Proc. Natl. Acad. Sci. USA **96:** 11041–11048.

C. elegans Sequencing Consortium, 1998 Genome sequence of the nematode *C. elegans*: a platform for investigating biology. Science **282:** 2012–2018.

Chou, P. Y., and G. D. Fasman, 1978 Prediction of the secondary structure of proteins from their amino acid sequence. Adv. Enzymol. **47:** 145–148.

Daum, G., G. Tuller, T. Nemec, C. Hrastnik, G. Balliano *et al.*, 1999 Systematic analysis of yeast strains with possible defects in lipid metabolism. Yeast **15:** 601–614.

Dawson, P. A., N. D. Ridgway, C. A. Slaughter, M. S. Brown and J. L. Goldstein, 1989a cDNA cloning and expression of oxysterol-binding protein, an oligomer with a potential leucine zipper. J. Biol. Chem. **264:** 16798–16803.

Dawson, P. A., D. R. Van Der Westhuyzen, J. L. Goldstein and M. S. Brown, 1989b Purification of oxysterol binding protein from hamster liver cytosol. J. Biol. Chem. **264:** 9046–9052.

Dimster-Denk, D., M. K. Thorsness and J. Rine, 1994 Feedback regulation of 3-hydroxy-3-methylglutaryl coenzyme A reductase in *Saccharomyces cerevisiae*. Mol. Biol. Cell **5:** 655–665.

Dimster-Denk, D., J. Rine, J. Phillip, S. Scherer, P. Cundiff *et al.*, 1999 Comprehensive evaluation of isoprenoid biosynthesis regulation in *Saccharomyces cerevisiae* utilizing the Genome Reporter Matrix. J. Lipid Res. **40:** 850–860.

Dutcher, S. K., 1981 Internuclear transfer of genetic information in *kar1-1/KAR1* heterokaryons in *S. cerevisiae*. Mol. Cell. Biol. **1:** 246–253.

Fang, M., B. G. Kearns, A. Gedvilaite, S. Kagiwada, M. Kearns *et al.*, 1996 Kes1p shares homology with human oxysterol binding protein and participates in a novel regulatory pathway for yeast Golgi-derived transport vesicle biogenesis. EMBO J. **15:** 6447–6459.

Fournier, M. V., F. C. Guimaraes, M. E. Paschoal, L. V. Ronco, M. G. Carvalho and A. B. Pardee, 1999 Identification of a gene encoding a human oxysterol-binding protein-homologue: a potential general molecular marker for blood dissemination of solid tumors. Cancer Res. **59:** 3748–3753.

Gaber, R. F., D. M. Copple, B. K. Kennedy, M. Vidal and M. Bard, 1989 The yeast gene *ERG6* is required for normal membrane function but is not essential for biosynthesis of the cell-cycle-sparking sterol. Mol. Cell. Biol. **9:** 3447–3456.

Goffeau, A., B. G. Barrell, H. Bussey, R. W. Davis, B. Dujon, *et al.*, 1996 Life with 6000 genes. Science **274:** 546–567.

Goldstein, J. L., and M. S. Brown, 1990 Regulation of the mevalonate pathway. Nature **343:** 425–430.

Hampton, R. Y., and J. Rine, 1994 Regulated degradation of HMG-CoA reductase, an integral membrane protein of the endoplasmic reticulum, in yeast. J. Cell Biol. **125:** 299–312.

Hemmings, B. A., 1997 PH domains—a universal membrane adapter. Science **275:** 1899.

Hildebrandt, E. R., and M. A. Hoyt, 2000 Mitotic motors in *Saccharomyces cerevisiae*. Biochim. Biophys. Acta **1496:** 99–116.

Hoyt, M. A., L. He, L. Totis and W. S. Saunders, 1993 Loss of function of *Saccharomyces cerevisiae* kinesin-related *CIN8* and *KIP1* is suppressed by *KAR3* motor domain mutants. Genetics **135:** 35–44.

Hull, C. M., and A. D. Johnson, 1999 Identification of a mating type-like locus in the asexual pathogenic yeast *Candida albicans*. Science **285:** 1271–1275.

Jiang, B., J. L. Brown, J. Sheraton, N. Fortin and H. Bussey, 1994 A new family of yeast genes implicated in ergosterol synthesis is related to the human oxysterol binding protein. Yeast **10:** 341–353.

Kandutsch, A. A., H. W. Chen and H.-J. Heiniger, 1978 Biological activity of some oxygenated sterols. Science **201:** 498–501.

Kyte, J., and R. F. Doolittle, 1982 A simple method for displaying the hydropathic character of a protein. J. Mol. Biol. **157:** 105–132.

Lagace, T. A., D. M. Byers, H. W. Cook and N. D. Ridgway, 1997 Abnormal cholesterol and cholesteryl ester synthesis in Chinese hamster ovary cells overexpressing the oxysterol binding protein is dependent on the pleckstrin homology domain. Biochem. J. **326:** 205–213.

Lange, Y., and T. L. Steck, 1998 Four cholesterol-sensing proteins. Curr. Opin. Struct. Biol. **8:** 435–439.

Lemmon, M. A., M. Falasca, K. M. Ferguson and J. Schlessinger, 1997 Regulatory recruitment of signaling molecules to the cell membrane by pleckstrin-homology domains. Trends Cell Biol. **7:** 237–242.

Levanon, D., C.-L. Hsieh, U. Francke, P. A. Dawson, N. D. Ridgway *et al.*, 1990 cDNA cloning of human oxysterol-binding protein and localization of the gene to human chromosome 11 and mouse chromosome 19. Genomics **7:** 65–74.

Levine, T. P., and S. Munro, 1998 The pleckstrin homology domain of oxysterol-binding protein recognizes a determinant specific to Golgi membranes. Curr. Biol. **8:** 729–739.

Li, X., S. M. Routt, Z. Xie, X. Cui, M. Fang *et al.*, 2000 Identification of a novel family of nonclassic yeast phosphatidylinositol transfer proteins whose function modulates phospholipase D activity and Sec14p-independent cell growth. Mol. Biol. Cell **11:** 1989–2005.

Lupas, A., 1996 Prediction and analysis of coiled-coil structures. Methods Enzymol. **266:** 513–525.

Nes, W. D., S. H. Xu and W. F. Haddon, 1989 Evidence for similarities and differences in the biosynthesis of fungal sterols. Steroids **53:** 533–558.

Ridgway, N. D., 2000 Interactions between metabolism and intracellular distribution of cholesterol and sphingomyelin. Biochim. Biophys. Acta **1484:** 129–141.

Ridgway, N. D., P. A. Dawson, Y. K. Ho, M. S. Brown and J. L.

Goldstein, 1992 Translocation of oxysterol binding protein to Golgi apparatus triggered by ligand binding. J. Cell Biol. **116:** 307–319.

Ridgway, N. D., T. A. Lagace, H. W. Cook and D. M. Byers, 1998 Differential effects of sphingomyelin hydrolysis and cholesterol transport on oxysterol-binding protein phosphorylation and Golgi localization. J. Biol. Chem. **273:** 31621–31628.

Robinson, J. S., D. J. Klionsky, L. M. Banta and S. D. Emr, 1988 Protein sorting in Saccharomyces cerevisiae: isolation of mutants defective in the delivery and processing of multiple vacuolar hydrolases. Mol. Cell. Biol. **8:** 4936–4948.

Russell, D. W., 1999 Nuclear orphan receptors control cholesterol catabolism. Cell **97:** 539–542.

Sambrook, J., E. F. Fritsch and T. Maniatis, 1989 *Molecular Cloning*, Ed. 2. Cold Spring Harbor Laboratory Press, Cold Spring Harbor, NY.

Saunders, W. S., and M. A. Hoyt, 1992 Kinesin-related proteins required for structural integrity of the mitotic spindle. Cell **70:** 451–458.

Schmalix, W. A., and W. Bandlow, 1994 *SWH1* from yeast encodes a candidate nuclear factor containing ankyrin repeats and showing homology to mammalian oxysterol-binding protein. Biochim. Biophys. Acta **1219:** 205–210.

Schroepfer, G. J., 2000 Oxysterols: modulators of cholesterol metabolism and other processes. Physiol. Rev. **80:** 361–554.

Sedgwick, S. G., and S. J. Smerdon, 1999 The ankyrin repeat: a diversity of interactions on a common structural framework. Trends Biochem. Sci. **24:** 311–316.

Sikorski, R. S., and P. Hieter, 1989 A system of shuttle vectors and yeast host strains designed for efficient manipulation of DNA in *Saccharomyces cerevisiae*. Genetics **122:** 19–27.

Storey, M. K., D. M. Byers, H. W. Cook and N. D. Ridgway, 1998 Cholesterol regulates oxysterol binding protein (OSBP) phosphorylation and Golgi localization in Chinese hamster ovary cells: correlation with stimulation of sphingomyelin synthesis by 25-hydroxycholesterol. Biochem. J. **336:** 247–256.

Taylor, F. R., S. E. Saucier, E. P. Shown, E. J. Parish and A. A. Kandutsch, 1984 Correlation between oxysterol binding to a cytosolic binding protein and potency in repression of HMG-CoA reductase. J. Biol. Chem. **259:** 12382–12387.

Vallen, E. A., M. A. Hiller, T. Y. Scherson and M. D. Rose, 1992 Separate domains of *KAR1* mediate distinct functions in mitosis and nuclear fusion. J. Cell Biol. **117:** 1277–1287.

Wach, A., A. Brachat, R. Pohlmann and P. Philippsen, 1994 New heterologous modules for classical or PCR-based gene disruptions in *Saccharomyces cerevisiae*. Yeast **10:** 1793–1808.

Walker-Caprioglio, H. M., J. M. MacKenzie and L. W. Parks, 1989 Antibodies to nystatin demonstrate polyene specificity and allow immunolabeling of sterols in *Saccharomyces cerevisiae*. Antimicrob. Agents Chemother. **33:** 2092–2095.

Woods, R. A., 1971 Nystatin-resistant mutants of yeast: alterations in sterol content. J. Bacteriol. **108:** 69–73.

Xinmin, L., Z. Xie and V. A. Bankaitis, 2000 Phosphatidylinositol/phosphatidylcholine transfer proteins in yeast. Biochim. Biophys. Acta **1486:** 55–71.

Zinser, E., C. C. Sperka-Gottlieb, E. V. Fasch, S. D. Kohlwein, F. Paltauf *et al.* 1991 Phospholipid synthesis and lipid composition of subcellular membranes in the unicellular eukaryote *Saccharomyces cerevisiae*. J. Bacteriol. **173:** 2026–2034.

Communicating editor: M. Johnston